A Simple Model of the Indonesian Throughflow and Its Composition

ROXANA C. WAJSOWICZ

The Institute for Low Temperature Science, Hokkaido University, Sapporo, Japan

(Manuscript received 27 March 1992, in final form 9 March 1993)

ABSTRACT

A simple analytical model of the closure of the wind-driven gyres in the tropical west Pacific is developed to illustrate the role of Halmahera and variations in the Pacific wind stress on the water mass composition of the flow from the Pacific to the Indian Ocean through the Indonesian archipelago—that is, the Indonesian Throughflow. The model is expressed in terms of the streamfunction, ψ, for the depth-integrated velocity field. There are three principal dynamical states, and therefore composition regimes. In the absence of Halmahera, the throughflow is composed of water wholly originating from the South Pacific (SP) if the streamfunction at the interior edge of the western boundary layer at the latitude of the northern tip of Papua New Guinea (PNG), ψ_N, is greater than that on the Asian continent, taken as zero, which is typically the situation in the Northern Hemisphere late summer. The throughflow is composed of water of wholly North Pacific origin (NP) if $\psi_N \leq \psi_A$, the value of the streamfunction on Australia–PNG, which corresponds to winter conditions. The throughflow is fed by both the fresh Mindanao Current and the saltier South Equatorial Current (SEC) otherwise. If Halmahera is taken into account, the criteria determining the composition regimes are modified. Its presence results in a fresher throughflow, 30% NP–70% SP compared with 100% SP, as ψ typically decreases northwards in the equatorial west Pacific. The result of averaging over perturbations in ψ_N, ψ_A is also considered.

Estimates of the throughflow composition from observed hydrography imply a predominantly NP source. A possible explanation is nonlinear retroflection of the SEC into the North Equatorial Countercurrent (NECC), which would lead to the throughflow being fed by the Mindanao Current for much of the year. However, the simple model predicts that a large amount of water of NP origin enters the Indonesian basins before exiting to feed the NECC, even when the throughflow is predicted to be wholly SP. Mixing within the basins would modify the composition of the NECC and throughflow. Different west Pacific states and their effect on the composition are investigated further with a flat-bottomed, homogeneous numerical general circulation model with a simplified geometry and climatological monthly mean forcing.

1. Introduction

In a recent note, Godfrey et al. (1993) point out an apparent inconsistency between the water mass properties of the Indonesian Throughflow and its source as predicted by Godfrey's (1989) Sverdrup model forced by Hellerman and Rosenstein's (1983) wind-stress climatology (henceforth referred to as HR data). Deductions based on salinity budgets led Gordon (1986) to suggest that the relatively fresh surface waters of the North Pacific are the source of the throughflow. Further evidence of a North Pacific origin is given by Lukas et al. (1991), who tracked buoys from the Mindanao Current region into the Indonesian seas. However, a Sverdrup model with vorticity dissipated at the latitude of creation in the western boundary layers and forced by HR data predicts a throughflow directly fed by the saltier South Equatorial Current (SEC). The streamline pattern in the west Pacific is sensitive to the wind-stress dataset used, as shown by Landsteiner et al. (1990). West Pacific streamline patterns generated by a Sverdrup model forced by The Florida State University (FSU) pseudo-wind stresses (Goldenberg and O'Brien 1981), University of Hawaii winds (Sadler et al. 1987), and Fleet Numerical Oceanographic Center's (FNOC) operational wind product would all give a throughflow of South Pacific (SP) origin. Godfrey et al. (1993) propose that the SEC retroflects into the North Equatorial Countercurrent (NECC) through either nonlinear or viscous processes.

The relative importance of advective effects, local precipitation, and mixing in determining the salinity distribution in the Indonesian seas, as shown by Gordon (1986), is difficult to assess and needs further investigation. In practice, it is likely that streamlines from both the Mindanao Current and SEC enter the Indonesian basins and considerable mixing occurs there. This has been demonstrated recently by Ffield and Gordon (1992) using a simple advective–diffusive model. They concluded that a flow of 10 Sv (Sv $\equiv 10^6$ m^3 s^{-1}) through the Makassar strait would have to be almost wholly of North Pacific (NP) origin, and a flow

Corresponding author address: Dr. Roxana C. Wajsowicz, Oceans and Ice Branch, NASA/Goddard Space Flight Center, Mail Code 971, Greenbelt, MD 20771.

(a) Regime I

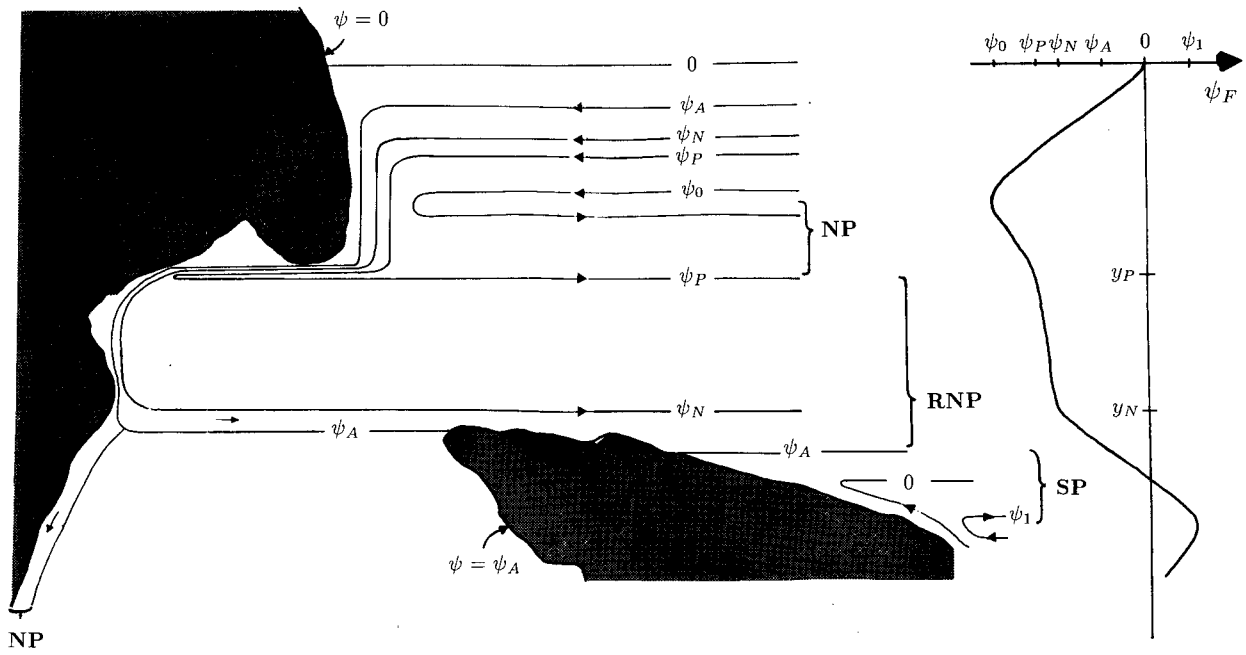

FIG. 1. Schematics of the streamfunction field in the absence of Halmahera for the analytical model with forcing field $\psi_F(y)$ shown on the right; scales are exaggerated to show details. The three regimes are as described in (2.2) and (2.3).

of 5 Sv through the Banda Sea would have to be an approximate mix of 75% NP to 25% SP origin to be consistent with observed residence times and an O(1 $cm^2 s^{-1}$) vertical diffusivity coefficient for salinity. Neither Godfrey et al. (1993) nor Ffield and Gordon (1992) considered the possibility that a large portion of the Mindanao Current could enter the Celebes Sea before exiting to make up the NECC. It would not contribute to the throughflow per se but could considerably freshen any SP component passing around Halmahera if there was significant horizontal mixing. Also, Godfrey et al.'s (1993) considerations did not take into account the presence of the island of Halmahera, just to the northwest of Papua New Guinea (PNG), whose northern tip is at about 3°N. If the circulation of the depth-integrated flow around its boundary matched that around Australia–PNG, then the implied SP component of the throughflow in a Sverdrup model would be reduced by 30%.

There is considerable variability in the currents of the western Pacific due to the seasonal movement of the intertropical convergence zone (ITCZ) and associated variation in the zonal component of the wind stress. The streamline pattern shown by Godfrey et al. (1993) represents the annual mean, but it is likely that the wind-driven gyres will close differently during the course of the year giving different relative compositions of NP and SP waters. There is also evidence that the throughflow magnitude varies seasonally, reaching a maximum in July and a minimum in February corresponding to the monsoon seasons (Wytrki 1987; Kindle et al. 1989). Therefore, the annual-mean throughflow composition will depend on its magnitude during a given dynamical regime and the fraction of a year that the ocean is in that regime, as well as mixing processes.

Factors influencing the magnitude of the throughflow and its water mass composition are investigated with a simple dynamical model developed in section 2. The model may be considered diagnostic in the sense that given the streamfunction at the interior edge of the western boundary layer at the latitude of the tips of PNG, Halmahera, and the Philippines and the value of the streamfunction on Australia and Halmahera, then the composition of the throughflow and NECC in the absence of mixing may be deduced. The time scale of validity of the model is determined by the assumed existence of a streamfunction representative of the upper-ocean velocity field, neglect of topographic effects, and by the values assigned to the various quantities. For example, if the streamfunction at the edge of the Pacific western boundary layer is assumed to be that given by Sverdrup dynamics, and the values on Australia–PNG and Halmahera are those given by Godfrey's (1989) Island Rule, then the model describes variations on time scales longer than a year, as discussed

(b) Regime II

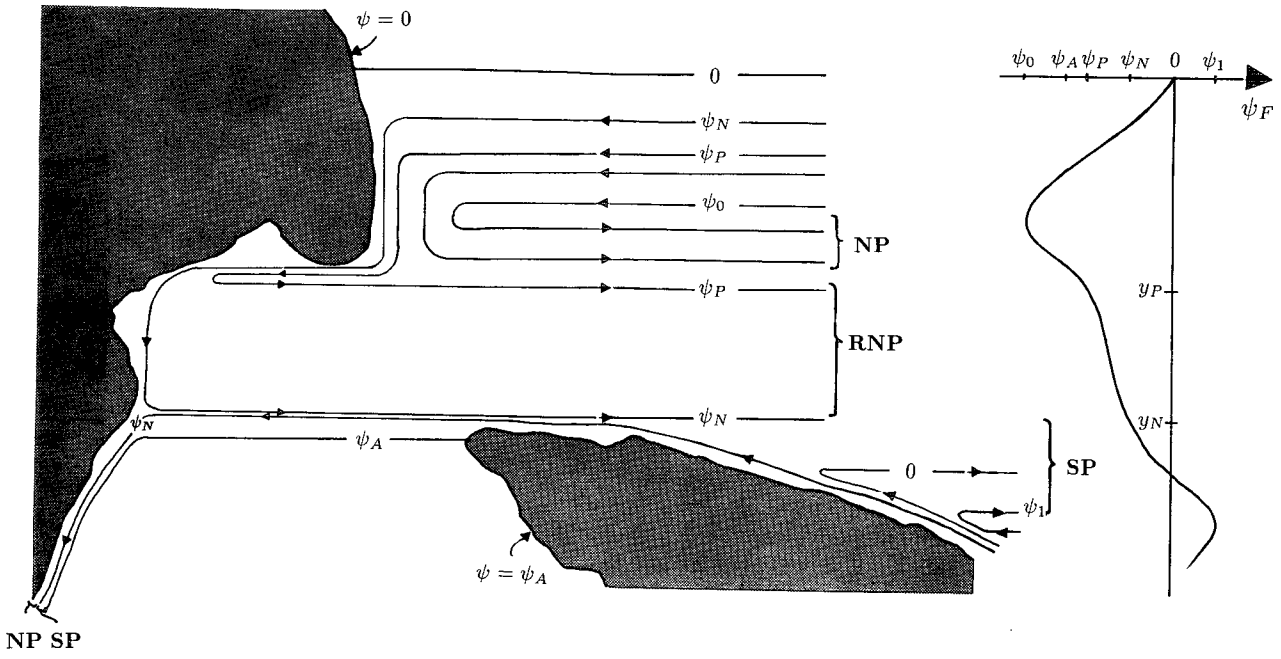

(c) Regime III

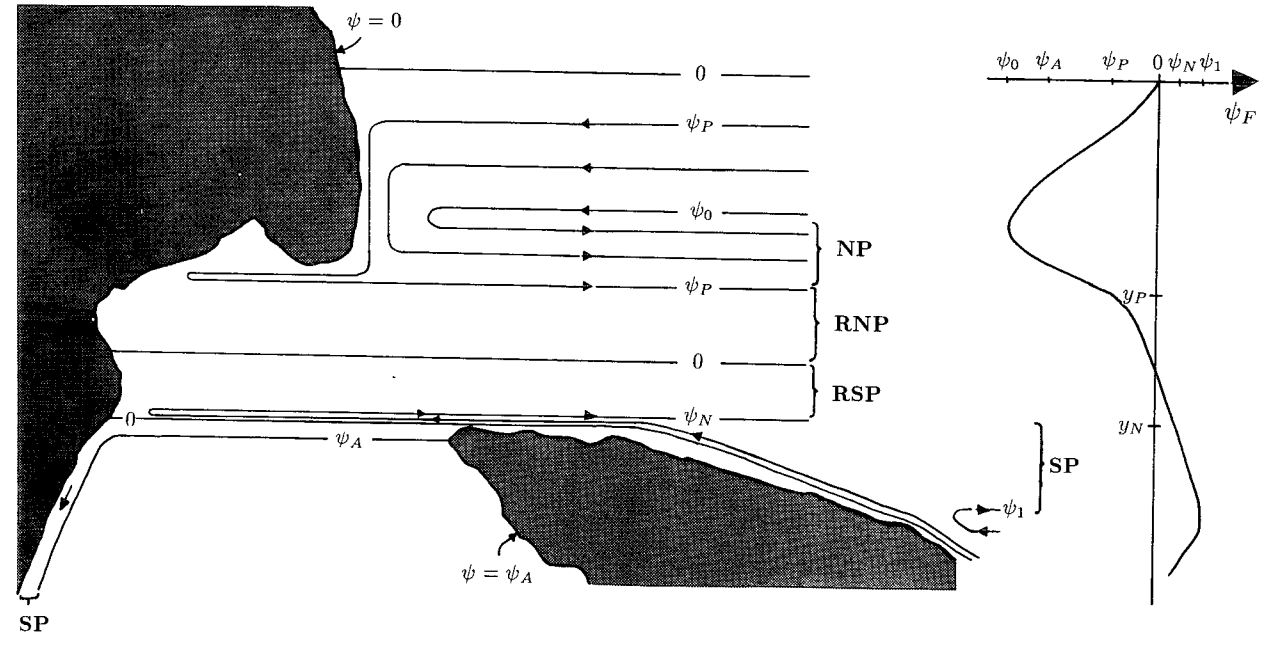

FIG. 1. (*Continued*)

by Wajsowicz (1993). Although the model described in section 2 is very simple and based on linear dynamics, it is inherently nonlinear when considering composition as an integral over time. This is explored further in section 3, where the variation in composition averaged over a cycle is considered as a function of the

mean and perturbation amplitudes of streamfunction at specific locations. Results from the simple model suggest that the annual mean composition could be of predominantly NP origin without invoking retroflection of the SEC into the NECC. A further investigation of viscous effects and states of the west Pacific using a simplified numerical general circulation model (GCM) is presented in section 4.

2. An analytical model of the throughflow composition

The existence of a streamfunction, ψ, for the depth-integrated velocity field may be deduced by vertically integrating the continuity equation and making the rigid-lid approximation ($w = 0$ at the surface). The streamfunction is given by

$$\psi_x = \int_{-H}^{0} v\,dz, \quad \psi_y = -\int_{-H}^{0} u\,dz,$$

where $z = -H(x, y)$ is the ocean floor. Assuming linear dynamics, and neglecting topographic effects and bottom stresses, the vorticity equation for the depth-integrated flow reduces to

$$\beta\psi_x = \text{curl}\,\frac{\boldsymbol{\tau}}{\rho_o} + \text{curl}\,\mathbf{F} \qquad (2.1)$$

on time scales greater than the barotropic–topographic Rossby adjustment scale. Frictional effects are represented by the term $\mathbf{F}$. If the water mass properties of the depth-integrated flow are representative of those for flow into the archipelago, then (2.1) could be used as a basis for a dynamical model of composition variations on seasonal time scales. A more realistic interpretation is that ψ is the upper-layer streamfunction in a two-layer model in which the lower layer is at rest and any topography is confined to the depth of the lower layer. In this case, (2.1) describes variations on time scales longer than the first baroclinic mode equatorial adjustment time scale—that is, ~280 days.

The essential elements of the simple dynamical model are the following:

(i) The streamfunction along a line spanning the equatorial region, ψ_F, and those on the islands of Australia–PNG and Halmahera, ψ_A, ψ_H, respectively, are assumed known.

(ii) Equation (2.1) reduces to $\psi_x = 0$ outside any western boundary layer west of the line on which ψ_F is specified.

(iii) Vorticity is destroyed at the latitude of creation within western boundary layers.

Therefore, the streamlines ψ = const are zonal west of the given line except in the western boundary layers, where ψ_x is of one sign. A consequence is that there may be infinitesimally thin zonal jets extending westward from the tips of each landmass.

In describing interannual variations, a suitable choice for ψ_F is the Sverdrup transport at the interior edge of the western boundary layers of Australia–PNG and the Philippines and a line connecting these points. Modeling seasonal variations is more tricky, and it is likely that only a qualitative impression can be achieved. If the Indonesian archipelago were at mid-latitudes, where the Coriolis parameter can be assumed constant over 10°–20° of latitude, then ψ could be reinterpreted as the geostrophic transport streamfunction at a representative depth. In the equatorial regions, such a reinterpretation is not valid, and ψ must remain the streamfunction of the depth-integrated flow above an approximate level of no motion. Suitable ψ_F would need to be constructed from details of the seasonal variations in the velocity fields.

a. No Halmahera

A schematic of the system considered is shown in Fig. 1. It is assumed that the streamfunction on Australia, $\psi_A < 0$, and the Mindanao low, $\psi_0 < 0$ and the high associated with the South Equatorial Current (SEC), $\psi_1 > 0$, where $\psi = 0$ is the value of ψ set as a boundary condition on the South American and Asian continents. Further, it is assumed that ψ_F decreases monotonically from the latitude of the northern tip of PNG, y_N to the southern tip of the Philippines at y_P, so that $\psi_0 < \psi_P < \psi_N < \psi_1$, where $\psi_N = \psi_F(y_N)$, $\psi_P = \psi_F(y_P)$. This is consistent with results from a Sverdrup model using climatological wind stresses. The manner in which the gyres close in the west Pacific will depend on the relative magnitudes of ψ_A, ψ_N, and ψ on the Philippines, which for the sake of simplicity is taken as the Asian continent value of 0. If $\psi_P \geq 0$, then no water of NP origin will enter the Indonesian seas, as the Mindanao Current will have separated from the coast before reaching the tip of the Philippines. If $\psi_P < 0$, then the Mindanao Current will transport $|\psi_P|$ of water of NP origin into the Indonesian seas. An amount $\{\min(\psi_N, 0) - \psi_P\}$, $(\psi_P < 0)$ will exit again between the latitudes y_P and y_N. If $\psi_N < \psi_A (< 0)$, then a further fraction $\{\psi_A - \psi_N\}$ will cross to the tip of PNG in a thin zonal jet and exit. Therefore, the amount of water of NP origin continuing south into the Indonesian seas to make up the throughflow is $\min\{\max(\psi_N, \psi_A), 0\}$. The total throughflow is $-\psi_A$, and the difference is made up of water of SP origin. If $\psi_N \leq \psi_A$, then the SEC will wholly separate from the Australia–PNG coast before reaching the tip of PNG. If $\psi_A < \psi_N$, then a zonal jet from the tip of PNG of magnitude $\{\psi_N - \psi_A\}$, containing water of SP origin, will enter the Indonesian seas. If $\psi_N < 0$, then it will all go to make up the throughflow, otherwise a fraction $-\psi_A$ will make up the throughflow and a fraction ψ_N will exit to make up the NECC. Hence, the Indonesian Throughflow composition is given by

$$\psi_{IT} = (-\psi')_{NP} + (\psi' - \psi_A)_{SP},$$
$$\psi' = \min\{\max(\psi_N, \psi_A), 0\}, \quad (2.2a)$$

where NP, SP denote water originating from the Mindanao Current and the SEC, respectively. The magnitude of the NECC is $\{\psi_1 - \psi_0\}$, and its composition is given by

$$\psi_{NECC} = (\hat{\psi} - \psi_0)_{NP} + (\psi_1 - \psi^*)_{SP} + (\psi' - \hat{\psi})_{RNP} + (\bar{\psi})_{RSP},$$
$$\hat{\psi} = \min(\psi_P, 0), \quad \psi^* = \max(\psi_N, \psi_A),$$
$$\bar{\psi} = \max(\psi_N, 0) = \psi^* - \psi', \quad (2.2b)$$

where RNP, RSP denote water of NP and SP origin, respectively, which have entered and circulated in the Indonesia seas before exiting. The expressions (2.2) are very concise, and it may be easier to think of the compositions in terms of the three regimes obtained by expanding the mins and maxs in (2.2), namely,

I: $(\psi_N \leq \psi_A)$

$$\psi_{IT} = (-\psi_A)_{NP}$$
$$\psi_{NECC} = (\psi_P - \psi_0)_{NP} + (\psi_1 - \psi_A)_{SP} + (\psi_A - \psi_P)_{RNP},$$

II: $(\psi_A < \psi_N < 0)$

$$\psi_{IT} = (-\psi_N)_{NP} + (\psi_N - \psi_A)_{SP}$$
$$\psi_{NECC} = (\psi_P - \psi_0)_{NP} + (\psi_1 - \psi_N)_{SP} + (\psi_N - \psi_P)_{RNP},$$

III: $(\psi_N \geq 0)$

$$\psi_{IT} = (-\psi_A)_{SP}$$
$$\psi_{NECC} = (\psi_P - \psi_0)_{NP} + (\psi_1 - \psi_N)_{SP} + (-\psi_P)_{RNP} + (\psi_N)_{RSP}, \quad \text{assuming} \quad \psi_P < 0, \quad (2.3)$$

which are illustrated in Fig. 1. In regime I, shown in Fig. 1a, the throughflow is of wholly NP origin. In regime III, shown in Fig. 1c, it is of wholly SP origin, and in regime II, shown in Fig. 1b, it is a mixture. If ψ is interpreted as the streamfunction of an upper-layer flow, then the regime boundaries are determined by the relative magnitudes of the depth-integrated pressure at the interior edge of the western boundary layer off the tip of PNG, the coastal value on PNG, and that on Asia. Regime I is loosely characterized by low pressure in the equatorial west Pacific corresponding to the Northern Hemisphere winter and a southerly location of the ITCZ, and regime III by high pressure corresponding to summer conditions with a northerly location of the ITCZ.

The above equations are quite general, in that given ψ_P, ψ_N, ψ_A, then the composition of the throughflow and NECC is determined, provided the dynamics at the entrance to the archipelago can be modeled as set out in conditions (i)–(iii). Specifically, it is not necessary to assume ψ_P, ψ_N are given by integrating (2.1), nor that ψ_A is given by Godfrey's (1989) Island Rule. Looking at Godfrey's (1989) Fig. 4, $\psi_N > 0$, hence the system is in regime III, and so the conclusion that a Sverdrup model would predict an annual-mean throughflow of SP origin.

The geometry considered in this example is very simple. The result is the same if islands to the west of PNG and the Philippines are included provided they are not directly exposed to the Pacific Ocean.

b. Including Halmahera

An island that does not satisfy this requirement is Halmahera; see Fig. 2. It has two effects on the throughflow composition. First, it could lead to an overall increase in the NP component of the throughflow, which is examined below. Second, depending on the relative magnitudes of ψ_A and ψ_H, the SEC component will pass either to the north or south of Halmahera. Although the effect cannot be distinguished in this purely dynamical model, if the SEC is diverted south of Halmahera into the Banda Sea, it will exit into the Indian Ocean subject to relatively little mixing. If it is diverted north of Halmahera, then it could mix with the water of NP origin flushing through the seas before exiting to make up the NECC.

A similar analysis can be made for the transport of the Mindanao Current and SEC as for the model in the absence of Halmahera. There are now many more regimes to consider. The throughflow composition is given by

$$\psi_{IT} = (-\Psi')_{NP} + (\Psi^* - \psi_A)_{SP} + (\bar{\Psi} - \Psi^*)_{RNP} + (\Psi' - \bar{\Psi})_{RSP}, \quad (2.4a)$$
$$\Psi' = \min\{\max(\psi_{HT}, \psi_A, \psi_H), 0\},$$
$$\Psi^* = \max\{\text{mid}(\psi_N, \psi_A, \psi_H), \psi_A\},$$
$$\bar{\Psi} = \max(\psi_A, \psi_H),$$

where $\psi_{HT} = \psi_F(y_{HT})$, and y_{HT} is the latitude of the northern tip of Halmahera. The NECC composition is given by

$$\psi_{NECC} = (\hat{\psi} - \psi_0)_{NP} + (\psi_1 - \psi^*)_{SP} + (\psi^* - \Psi'' + \Psi' - \hat{\psi})_{RNP} + (\Psi^{**})_{RSP} + (\Psi'' - \Psi' - \Psi^{**})_{WBL}, \quad (2.4b)$$
$$\hat{\psi} = \min(\psi_P, 0), \quad \psi^* = \max(\psi_N, \psi_A),$$
$$\Psi'' = \max(\psi_N, \psi_A, \psi_H), \quad \Psi^{**} = \max(\psi_{HT}, 0).$$

The four basic regimes found in realizations of the simple model in the next section may be written explicitly as follows:

I: ($\psi_{HT} \leqslant \bar{\Psi}$ and $\psi_A \geqslant \psi^{**}$)

$$\psi_{IT} = (-\bar{\Psi})_{NP} + (\bar{\Psi} - \psi_A)_{RNP}$$

$$\psi_{NECC} = (\psi_P - \psi_0)_{NP} + (\psi_1 - \psi_A)_{SP} + (\psi_A - \psi_P)_{RNP},$$

IIa: ($\psi_N, \psi_H > \psi_A, \psi_{HT}$)

$$\psi_{IT} = (-\psi_H)_{NP} + (\psi^{**} - \psi_A)_{SP} + (\psi_H - \psi^{**})_{RNP}$$

$$\psi_{NECC} = (\psi_P - \psi_0)_{NP} + (\psi_1 - \psi_N)_{SP} + (\psi^{**} - \psi_P)_{RNP} + (\psi_N - \psi^{**})_{WBL},$$

IIb: ($0 > \psi_{HT} > \psi_A, \psi_H$)

$$\psi_{IT} = (-\psi_{HT})_{NP} + (\bar{\Psi} - \psi_A)_{SP} + (\psi_{HT} - \bar{\Psi})_{RSP}$$

$$\psi_{NECC} = (\psi_P - \psi_0)_{NP} + (\psi_1 - \psi_N)_{SP} + (\psi_{HT} - \psi_P)_{RNP} + (\psi_N - \psi_{HT})_{WBL},$$

III: ($\psi_{HT} \geqslant 0$)

$$\psi_{IT} = (\bar{\Psi} - \psi_A)_{SP} + (-\bar{\Psi})_{RSP}$$

$$\psi_{NECC} = (\psi_P - \psi_0)_{NP} + (\psi_1 - \psi_N)_{SP} + (-\psi_P)_{RNP} + (\psi_{HT})_{RSP} + (\psi_N - \psi_{HT})_{WBL}, \quad (2.5)$$

where $\bar{\Psi} = \max(\psi_A, \psi_H)$ and $\psi^{**} = \min(\psi_H, \psi_N)$. Regimes I and III are shown in Fig. 2. From Godfrey et al. (1993), $\psi_{HT} \simeq -5$ Sv, $\psi_A \simeq -15$ Sv, and $\psi_N > 0$. The value of ψ on Halmahera may be estimated from the multiple, overlapping Island Rule derived in Wajsowicz (1993), which gives $\psi_H \sim -5$ Sv. Hence, the ocean is on the border of regimes IIa and IIb of (2.5), with a composition of 33% NP and 67% SP origin. If $\psi_H \approx \psi_A \approx -15$ Sv and $\psi_{HT} \approx -5$ Sv, then the system is in regime IIb. The composition will still be of 33% NP and 67% SP origin, but now the SP component will pass north of Halmahera and enter the Celebes Sea, and therefore is classified as RSP.

3. Realizations of the analytical model

Before investigating the effect of fluctuations in ψ_N, ψ_{HT} on the average throughflow composition in (b), it is useful to first demonstrate conditions under which the various regimes given by (2.2)–(2.5) arise, in particular those for the model including Halmahera.

a. *Sverdrup states corresponding to different positions of the ITCZ*

Suppose ψ_F takes the simple form

$$\psi_F(y) = \begin{cases} \psi_0 \sin k_0(y - y_0), & y > y_0 \\ \psi_1 \sin k_1(y - y_1), & y_0 \geqslant y \geqslant y_1 \\ \psi_2 \sin k_2(y - y_2), & y < y_1, \end{cases} \quad (3.1)$$

where

$$y_1 = y_0 - \pi/k_1, \quad y_2 = y_1 - \pi/k_2.$$

The above is suggested by the Sverdrup transport generated by the climatological wind stress used to force the GCM in the next section and shown later in Fig. 8. The latitude of the zero wind-stress curl line in the equatorial regions is y_0. Varying y_0 in (3.1) could correspond to simulating interannual variations in the ITCZ.

1) No Halmahera

The result of varying y_0 from 5°S to 5°N, and taking $\psi_0 = -25$ Sv, $\psi_1 = 15$ Sv, $\psi_2 = -40$ Sv, $k_0 = \pi/20°$ of latitude, $k_1 = \pi/15°$, $k_2 = \pi/40°$ is shown in Fig. 3a. The values of y_P and y_N are 5°N and 1°N, respectively. The value of ψ_A is specified as the average value for the cycle in y_0 as determined by Godfrey's (1989) Island Rule, which on ignoring the contribution from the integral of the alongshore wind stress around Australia–PNG reduces to

$$\psi_A = -\frac{1}{(y_N - y_S)} \int_{y_S}^{y_N} \psi_F dy, \quad (3.2)$$

where y_N, y_S are the latitudes of the northern and southern tips of Australia–PNG, respectively (Wajsowicz 1993). If ψ_A were given by (3.2) at each point in the cycle, then $|\psi_A|$ would increase almost linearly from 13 Sv to 19 Sv as y_0 increased from 5°S to 5°N. The system goes through regimes I, II, and III, as described in (2.3), as ψ_N increases from less than ψ_A to greater than zero. The NP composition of the throughflow decreases from 100% to zero. The NECC composition varies from 80% SP–20% RNP to an almost equal mix of SP, RNP, and NP for $y_0 = 1°$N and onto 60% NP–10% RNP–30% RSP. The resulting water origin fractions given by summing over a cycle of movement in y_0 are given in Table 1 for the throughflow and Table 2 for the NECC. In Fig. 3, the x axis is y_0, but may also be thought of as *time,* if it is assumed y_0 moves northwards uniformly with time.

In the next section, a simplified ocean GCM is spun up with HR data to show the different Sverdrup states achieved if the wind forcing were a perpetual January, February, and so on. A simplified representation of these states, and the changes between them, is given by setting the amplitudes of ψ_0, ψ_1, ψ_2 in (3.1) to

$$\psi_0 = \overline{\psi_0} + \hat{\psi}_0 \sin \frac{\pi}{L} y_0,$$

$$\psi_1 = \overline{\psi_1} + \hat{\psi}_1 \sin \frac{\pi}{L} y_0,$$

$$\psi_2 = \overline{\psi_2} + \hat{\psi}_2 \sin \frac{\pi}{L} y_0, \quad (3.3)$$

where $-L/2 < y_0 < L/2$. The result of varying y_0 from 5°S to 5°N, that is, $L = 10°$ of latitude, and taking $\overline{\psi_0} = -25$ Sv, $\hat{\psi}_0 = 5$ Sv, $k_0 = \pi/20°$, $\overline{\psi_1} = 15$ Sv, $\hat{\psi}_1 = 5$ Sv, $k_1 = \pi/15°$, $\overline{\psi_2} = -40$ Sv, $\hat{\psi}_2 = 10$ Sv, $k_2 = \pi/$

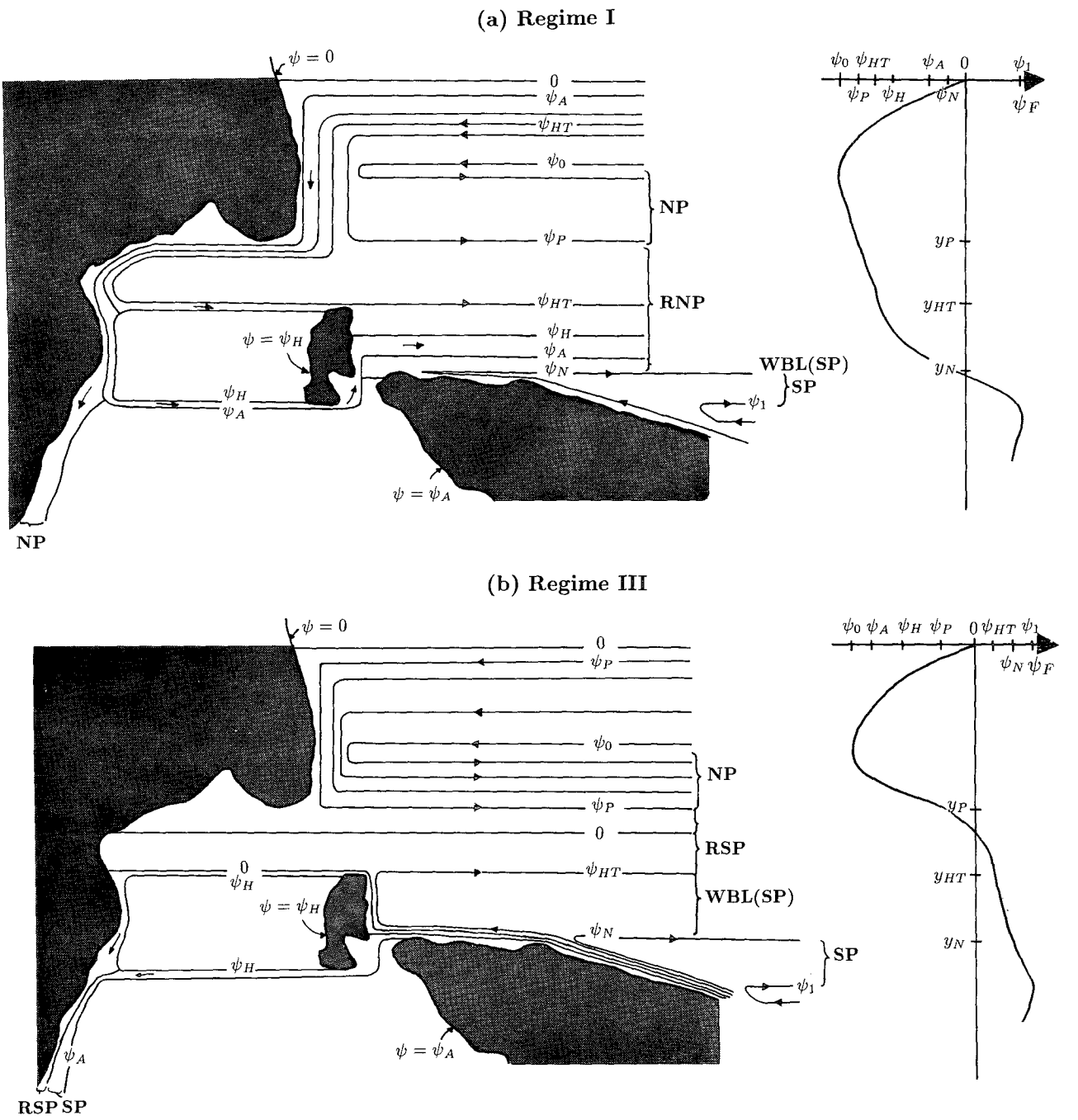

FIG. 2. As in Fig. 1 but including Halmahera. Only two regimes are shown for a throughflow of (a) wholly NP origin and (b) wholly SP origin. They are as described in (2.4) and (2.5).

40°, is shown in Fig. 3b. The mean value of ψ_A is as given by the Island Rule, and a perturbation of amplitude 50% of the mean has been imposed giving a maximum throughflow when y_0 is farthest north. If ψ_A were calculated from (3.2) at each point in the cycle, then it would decrease sinusoidally from 18.5 Sv at $y_0 = 3.5°$S to 12.5 Sv at $y_0 = 3.5°$N. The period of ψ_A is less than that of the highs and lows, L, and the average of ψ_A over a cycle is less than that in the model with no perturbation, although the averages of ψ_0, ψ_1, ψ_2 are the same. This is because (3.2) is nonlinear in y_0, and it suggests that in a more complex model, or the real oceans, the interannual variations in throughflow magnitude will not be

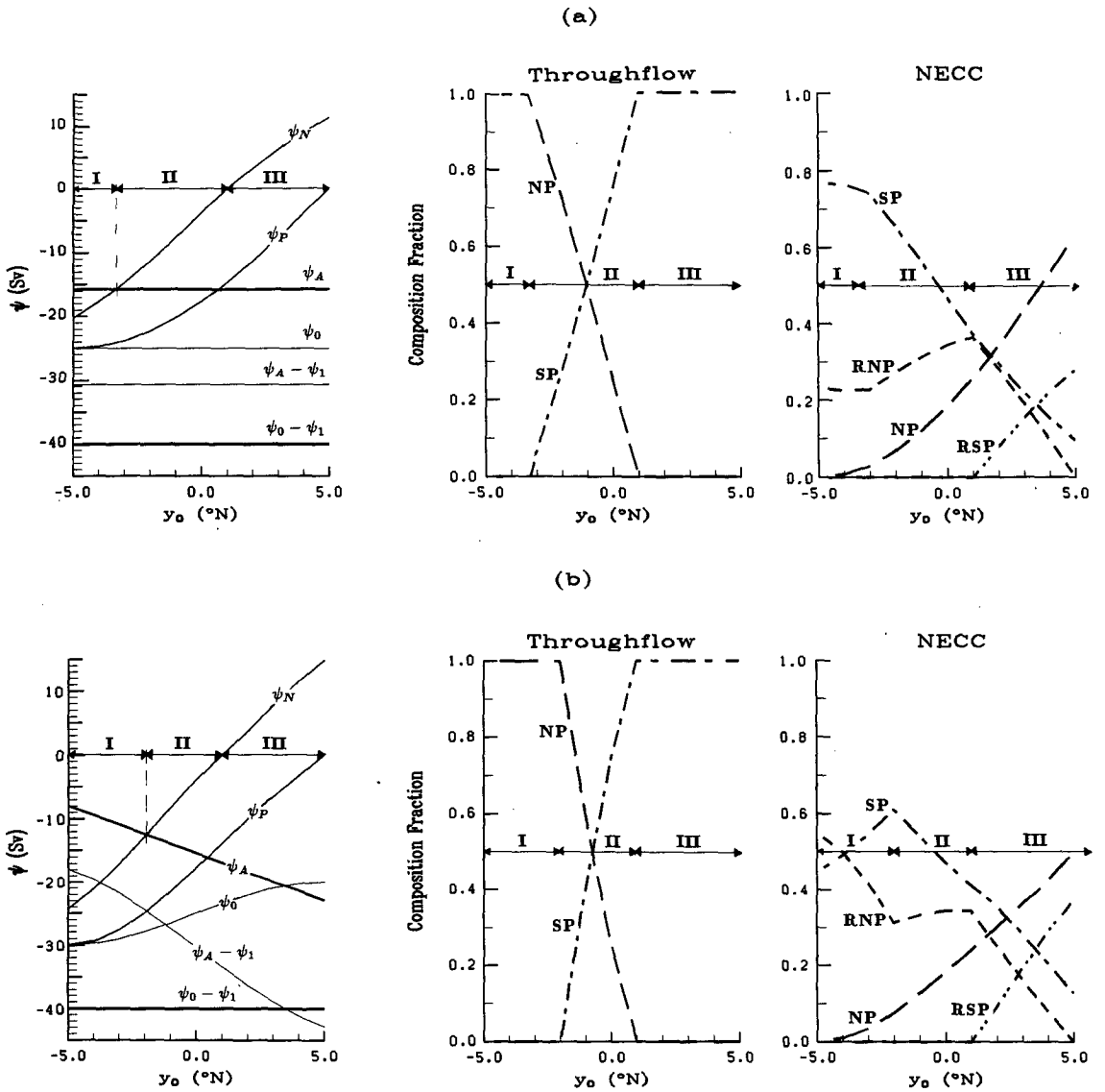

FIG. 3. (a) Case NH1: no Halmahera, and fixed magnitudes for $\psi_0, \psi_1, \psi_2, \psi_A$. (b) Case NH2: no Halmahera, and varying magnitudes for $\psi_0, \psi_1, \psi_2, \psi_A$. The variation in ψ_N, ψ_P as y_0 is varied is shown along with the magnitudes of $\psi_{IT}(\equiv -\psi_A)$, ψ_{NECC} $(\equiv \psi_0 - \psi_1)$ and the magnitude of the Mindanao Current ψ_0, and SEC$(\equiv \psi_A - \psi_1)$, in the leftmost plot. Also plotted are the compositions of the Indonesian Throughflow as a fraction of ψ_{IT} and of the NECC as a fraction of ψ_{NECC}. The water masses distinguished are NP (long dash), SP (dot-dash), denoting water masses directly fed by the Mindanao Current and SEC, respectively; RNP (short dash), RSP (double dot-dash), denoting water masses fed by the Mindanao Current and SEC after circulating in the Indonesian Basin.

strongly correlated with those of the SEC high, for example.

The main contrast with the previous example is that regime I exists for a greater extent of y_0. The Mindanao Current is much larger and SEC much smaller than in Fig. 3a during this phase, and this is reflected in the different composition of the NECC. The effect on the throughflow composition averaged over the cycle has been surprisingly small. The mix has gone from 40% NP–60% SP to 30% NP–70% SP; see Table 1.

2) INCLUDING HALMAHERA

The result of including Halmahera between 1°S and 3°N in the scenario of Fig. 3a is shown in Fig. 4a. The circulation around Halmahera is set to that around Australia. There is a much larger range of y_0 for which the model is in regime I, since it is now determined by $\psi_{HT} < \psi_A$; if $\psi_A \equiv \psi_H$, then regime IIa in (2.5) does not exist and is replaced by regime I. All of the SP component feeding the throughflow has passed north

TABLE 1. Composition of throughflow averaged over a cycle of the simple model (in Sv and % of $\overline{\psi_{IT}}$).

	NP	SP	RNP	RSP
		No Halmahera		
NH1: Fixed	6.28 (40.0%)	9.42 (60.0%)	—	—
NH2: Oscillatory	4.79 (31.1%)	10.61 (68.9%)	—	—
		Halmahera		
H1: Fixed	9.14 (58.2%)	0	0	6.56 (41.8%)
H2: ψ_A Oscillatory	6.82 (43.5%)	4.71 (30.0%)	≃0	4.16 (26.5%)

$\overline{\psi_0} = -25$	$k_0 = \pi/20°$	$\hat{\psi}_0 = 0$	$= 5$	$\overline{\psi_A} = -15.70$	$\overline{\psi_H} = \overline{\psi_A}$
$\overline{\psi_1} = 15$	$k_1 = \pi/15°$	$\hat{\psi}_1 = 0$	$= 5$	$= -15.40$ in NH2	$= -11.47$ in H2
$\overline{\psi_2} = -40$	$k_2 = \pi/40°$	$\hat{\psi}_2 = 0$	$= 10$ in NH2	$\hat{\psi}_A = 0$ $= 7.5$ in NH2 & H2	$\hat{\psi}_H = 0$
$\overline{\psi_N} = -4.22$ $= -4.47$ in NH2		$\overline{\psi_{HT}} = -10.22$		$\overline{\psi_P} = -15.58$ $= -16.78$ in NH2	

of Halmahera into the Celebes Sea. The NP fraction of the throughflow averaged over a cycle has increased to almost 60%. The effect of letting ψ_A vary but keeping other quantities fixed is shown in Fig. 4b. The circulation around Halmahera is given by the multiple, overlapping Island Rule derived in Wajsowicz (1993), which, ignoring the local forcing around Halmahera, reduces to

$$\psi_H = \frac{1}{(y_{HT} - y_{HB})} \int_{y_N}^{y_{HT}} \psi_F dy + \left(\frac{y_N - y_{HB}}{y_{HT} - y_{HB}}\right)\psi_A, \tag{3.4}$$

where y_{HT}, y_{HB} are the latitudes of the northern and southern tips of Halmahera, respectively. All four regimes described in (2.5) are now found. The component of the throughflow of SP origin is roughly equally divided between that entering the Celebes Sea first and that passing directly into the Banda Sea. The result of averaging over a cycle of y_0 is given in Tables 1 and 2.

b. *Time averages of sinusoidal perturbations*

The above examples illustrated the various regimes possible for a selection of ocean states. The forcing streamfunction, ψ_F, does not need to be specified at all latitudes. The relevant values for determining the composition of the throughflow are just ψ_A, ψ_N in the absence of Halmahera and ψ_A, ψ_H, ψ_N, ψ_{HT} if Halmahera is included. The west Pacific shows considerable variability on many time scales. An impression of the effect of this on the composition was given by the averages over y_0 detailed in Tables 1 and 2. A more formal exploration of the dependency of composition on the variability of ψ_N, ψ_A is presented below.

1) NO HALMAHERA

Suppose ψ_A, ψ_N vary sinusoidally with time about mean values and are 180° out of phase. For the seasonal cycle, this corresponds to the general notion that the throughflow $-\psi_A$ is a maximum (minimum) in the Northern Hemisphere summer/fall (winter/spring) when the pressure in the equatorial west Pacific is high (low). Nondimensionalizing amplitudes on the mean of $-\psi_A$, and denoting nondimensional quantities by ′, then

$$\psi'_A = -1 + a\cos t', \tag{3.5a}$$

$$\psi'_N = R - b\cos t', \tag{3.5b}$$

TABLE 2. Composition of NECC averaged over a cycle of the simple model (in Sv and % of $\overline{\psi_{NECC}} = \overline{\psi_1} - \overline{\psi_0} = 40$ Sv).

	NP	SP	RNP	RSP	WBL(SP)
			No Halmahera		
NH1	9.43 (23.6%)	18.63 (46.6%)	9.29 (23.2%)	2.65 (6.6%)	—
NH2	8.23 (20.6%)	16.34 (40.9%)	11.98 (29.9%)	3.45 (8.6%)	—
			Halmahera		
H1	9.43 (23.6%)	18.63 (46.6%)	6.44 (16.1%)	0.83 (2.0%)	4.67 (11.7%)
H2	"	17.08 (42.7%)	8.76 (21.9%)	"	3.90 (9.8%)

where t has been nondimensionalized on the frequency, R is the nondimensional mean of ψ_N, and a, $b(\geq 0)$ are the nondimensional amplitudes of the perturbations in ψ_A, ψ_N, respectively. Substituting in (2.2a) and averaging over a period yields an average NP fraction for the throughflow of

$$\overline{(\psi_{IT})}_{NP} = \frac{1}{\pi}(m - a\sin m) + \frac{1}{\pi}\{R(m-n) - b(\sin m - \sin n)\}, \quad (3.6a)$$

where

$$m = \begin{cases} 0, & a+b < 1+R \\ \cos^{-1}\dfrac{(1+R)}{(a+b)}, & a+b \geq |1+R| \\ \pi, & a+b < -(1+R) \end{cases},$$

$$n = \begin{cases} \pi, & b < -R \\ \cos^{-1}\dfrac{R}{b}, & b \geq |R| \\ 0, & b < R \end{cases}. \quad (3.6b)$$

It has been assumed that $a \leq 1$, so that the throughflow is *into* the Indian Ocean; that is, $\psi_A \leq 0$ throughout the cycle. The system spends from $t' = 0$ to m in regime I, from $t' = m$ to n in II, and from $t' = n$ to π in III; the cycle is symmetric about $t' = \pi$. The results are illustrated in Fig. 5 for $R = 0.3, 0.0, -0.3, -1.3$ for a, b ranging from 0 to 1. Recall from (2.3), if there were no variability in the west Pacific, that is, $a, b \equiv 0$, then $(\psi_{IT})_{NP} = 1$ for $R \leq -1$, $-R$ for $-1 \leq R \leq 0$, and 0 for $R \geq 0$.

Looking first at Fig. 5a for $R = 0.3$, there are three regions. If $b < R$, then $\psi_N > 0$ throughout the cycle, and the system will always be in regime III, so there will be no NP component to the throughflow. This corresponds to the lower third of the figure. If $b > R$, $a + b < 1 + R$, then $\psi_A < \psi_N$ throughout the cycle, and the system will be in regimes II and III during the cycle. The magnitude of the NP component will be $(-Rn + b\sin n)/\pi$, and so independent of a, the amplitude of the time-varying component of ψ_A. This corresponds to the upper left-hand side of Fig. 5a. If $b > R$, $a + b > 1 + R$, then the system will be in each of the three regimes during the cycle; this corresponds to the upper right-hand side of Fig. 5a. If $R = 0$, corresponding to a mean $\psi_N = 0$, then the region of regime III only is confined to the a axis (see Fig. 5b). The nonlinear nature of the system is well illustrated by this figure. Although the mean of ψ_N is zero, there will be a nonzero component of NP water provided b is nonzero. Kindle et al.'s (1989) calculations suggest that the effect of the monsoons is represented by taking $a \approx 2/3$, and $R \approx 0$. Estimating b is more difficult. Seasonal variations in the equatorial currents exceed 10 Sv, which suggests b may be as large as O(1). For $0 \leq b \leq 1/3$, the fraction of NP water varies rapidly from 0% to 11%. For $b > 1/3$, the fraction is relatively insensitive to b as $b \to \infty$. The maximum NP fraction is $1/2 - a/\pi$, and is obtained by letting $b \to \infty$ in (3.6), so that $m, n \to \pi/2$. Turning to Fig. 5c for $R = -0.3$, there are two new regions for $b < -R$. The fraction is a constant equal to $-R$ for the region $b \leq -R$, $a + b \leq 1 + R$; the system is in regime II throughout the cycle. In the region on the lower right-hand side of Fig. 5c, the system is in regimes I and II through the cycle, and the fraction of NP averaged over a cycle is just a function of $(a + b)$. For $a \simeq 2/3$, the NP composition decreases from 30% to 25% as b increases from 0 to about 0.4, and then increases to about 30% as $b \to \infty$. If $R \leq -1$, then it is possible for the throughflow to be 100% NP water. This occurs if the amplitudes of the perturbations to ψ_A, ψ_N are such that $a + b \leq -R - 1$, so that the system is in regime I for the whole cycle, see Fig. 5d. For $a \simeq 2/3$, the composition would decrease from 91% to 61% NP component as b increases from 0 to 1. The fraction is very sensitive to the choice of R, and for a given a, the sensitivity to the choice of b increases as R decreases. In interpreting Fig. 5, it is useful to note that points lying on the lines $(a + b)$ = const have spent the same amount of time in regime I, and those lying on b = const have spent the same amount of time in regime III.

2) Including Halmahera

Suppose the circulation around Halmahera is in phase with that around Australia–PNG, and is given by

$$\psi'_H = -H + h\cos t'. \quad (3.7)$$

Figure 5 can be reinterpreted for the case including Halmahera if R and b are reinterpreted as the mean and perturbation amplitudes of ψ_{HT} and $H \equiv 1$, $h \equiv a$. Since $\overline{\psi_{HT}}$ will typically be less than $\overline{\psi_N}$, then to compare the compositions with and without Halmahera Fig. 5b should be compared with Fig. 5a, and so on. Suppose $\overline{\psi_N'} \sim 0$, $\overline{\psi_{HT}'} \sim -0.3$, and $a \approx 2/3$, then from Fig. 5b, in the absence of Halmahera, the NP fraction would increase from 0% to 19% as b increases from 0 to 1. From Fig. 5c, if Halmahera is included, then the fraction decreases from 27% to 17% as b, now interpreted as the nondimensional amplitude of the perturbation in ψ_{HT}, increases from 0 to 1.

The effect of varying H, h is shown in Fig. 6, which should be compared with corresponding contour maps in Fig. 5. The plots are for different values of R but with $H = 0.75$, which is a fraction predicted by the multiple, overlapping Island Rule derived in Wajsowicz (1993) for a Sverdrup model. The amplitude of the temporal perturbation h is taken equal to a except when it would imply that $\psi_H > 0$ at some point in the cycle, in which case $h = H$. The parameter ψ_N does not enter

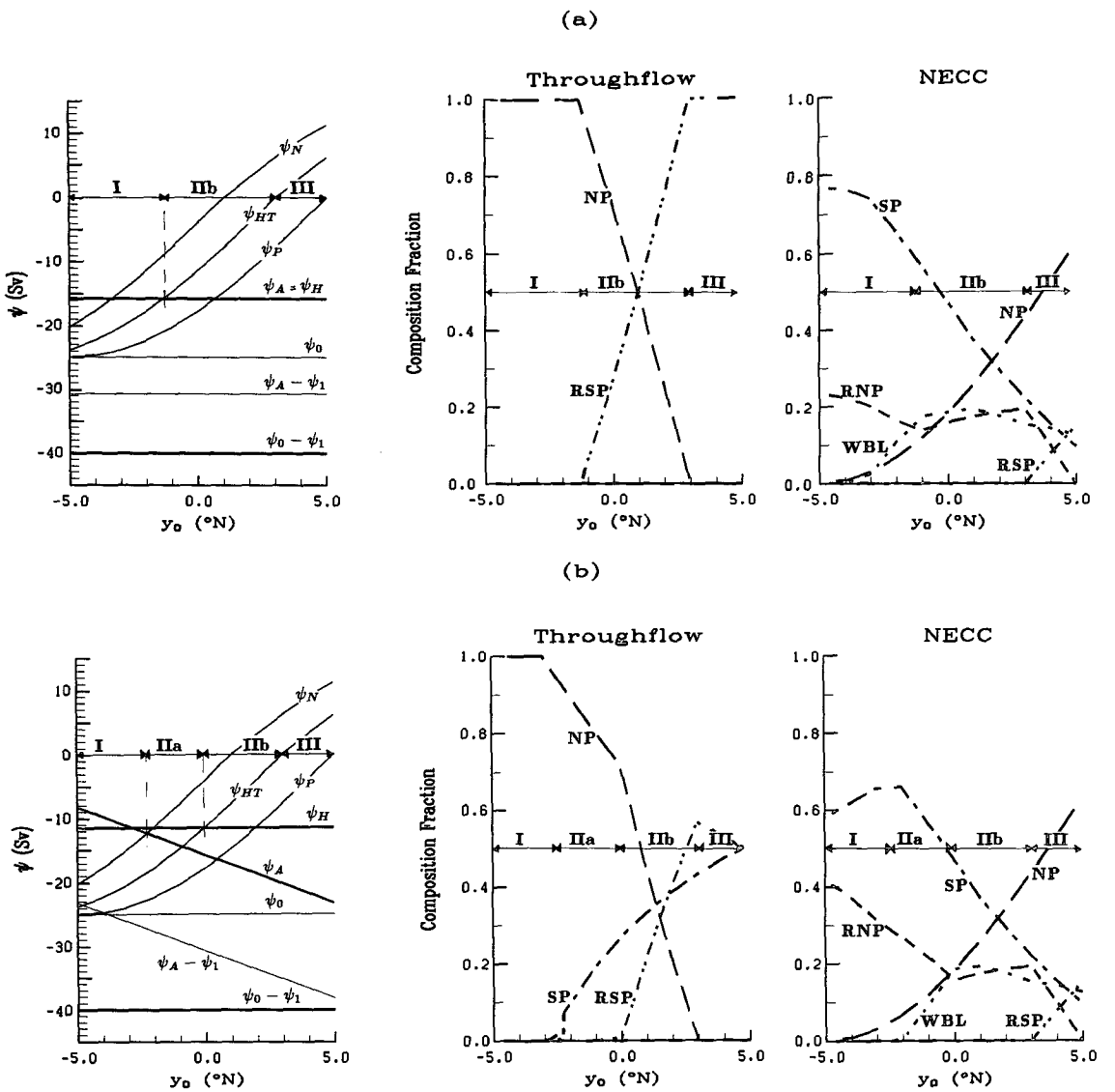

FIG. 4. As in Fig. 3 but for examples including Halmahera. (a) Case H1: including Halmahera and fixed ψ_0, ψ_1, ψ_2, $\psi_A = \psi_H$. (b) Case H2: including Halmahera, fixed magnitudes for ψ_0, ψ_1, ψ_2, ψ_H, and varying ψ_A. Halmahera is assumed to lie between 1°S and 3°N, so y_{HT} = 3°N. In this case, SP (dot-dash) denotes flow south of Halmahera, and RSP (double dot-dash) denotes flow north of Halmahera. A further component, WBL (dotted), is distinguished, which denotes SEC water from Halmahera's western boundary layer.

the problem provided it is assumed that the value of ψ_N is such that $\text{mid}(\psi_A, \psi_H, \psi_N) \neq \psi_N$. In all the plots, the introduction of regime I is now given by $h + b > R + H$. The introduction of regime III is still given by $b > -R$. The composition fraction for $h + b \leq R + H$, $R \geq -H$ is independent of the presence of Halmahera. If $R < -H$, then the composition fraction in the regime I–only region is limited to H, if $H < 1$. The effect of increasing h will be to steepen the line $h + b = |R + H|$, therefore an increase in the amplitude of the variability of the circulation around Halmahera will lead typically to a decrease in NP component of the throughflow averaged over a cycle. Looking at Fig. 6c for $R = -0.3$, if $a \approx 2/3$, then the fraction decreases from 26% to 16% as b increases from 0 to 1. If R were as low as -1.3, Fig. 6d, then the fraction would decrease from 73% to 47%.

If the throughflow composition is determined purely by dynamical conditions, then the simple model of section 2, whose properties have been explored above, suggests that to model the throughflow composition accurately in the annual mean, all time scales need to be resolved or the unresolved processes parameterized; for example, tidal fluctuation could be important. Of

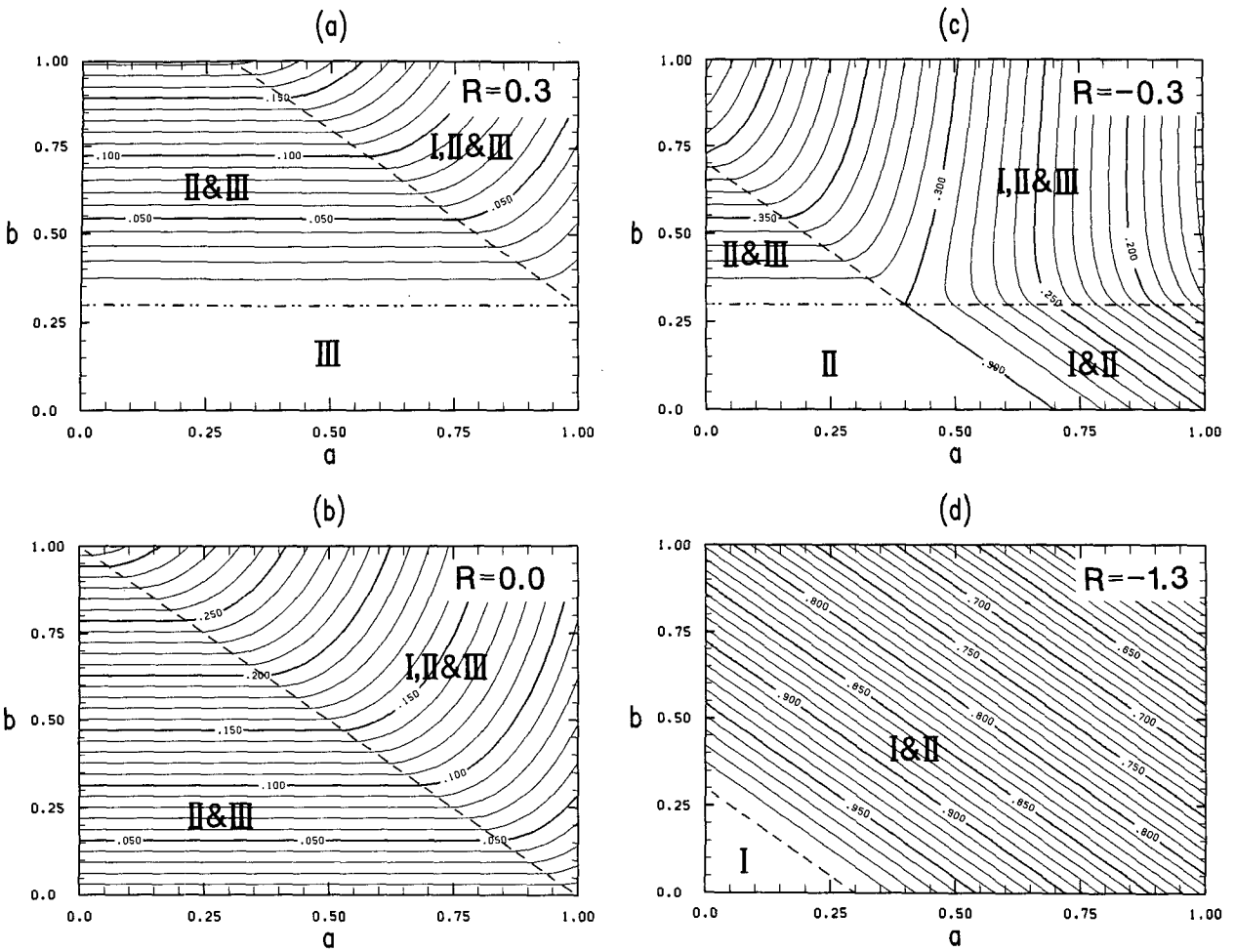

FIG. 5. The fraction of NP water mass in the throughflow (no Halmahera) averaged over a cycle as given by (3.6) is contoured as a function of a, b the perturbation amplitudes of ψ_A, ψ_N, respectively, for a given value of R, the mean value of ψ_N. Quantities have been nondimensionalized on the mean value of $-\psi_A$. In (a) $R = 0.3$, (b) $R = 0.0$, (c) $R = -0.3$, (d) $R = -1.3$. For $R > 0$, the basic regime is III. Time is spent in regime II if $b > R$, and in regime I if $a + b > 1 + R$. For $0 \geqslant R \geqslant -1$, the basic regime is II. Time is spent in regime III if $b > -R$, and in I if $a + b > 1 + R$. For $R < -1$, the basic regime is I. Time is spent in regime II if $a + b > -(1 + R)$, and in III only if $b > -R$. The line $a + b = |1 + R|$ is denoted by short dash, and the line $b = |R|$ by double dot–dash.

course, the role of horizontal mixing in models is to represent unresolved processes, which means temporal as well as spatial. Therefore, in a numerical general circulation model with climatological mean forcing, for example, the role of the horizontal "eddy" viscosity in the west Pacific is to produce a closure of the wind-driven gyres, which is an average of all the different states that have occurred over time scales not resolved explicitly by the model nor resolved in the forcing field specified. A GCM is designed to simulate the real oceans, so even if a steady wind-stress field is specified, the ocean state simulated is meant to be representative of the average of all the states that would exist if all the high-frequency fluctuations in the wind field had been included. Returning to Godfrey et al.'s (1993) paradox, GCMs like those of Hirst and Godfrey (1993) and Semtner and Chervin (1988) produce viscous retroflection so that the gyres close with the streamlines from the Mindanao Current forming the throughflow in order to get a consistent dynamical and physical interpretation of the annual mean state. Feeding by the Mindanao Current does not imply that the dynamical source of the throughflow is associated with the North Pacific wind stress; it can still be the South Pacific wind-stress curl as given by Sverdrup dynamics. Interannual variations in the South Pacific wind-stress curl will produce variations in the throughflow; variations in the North Pacific curl will only produce variations in composition and not in magnitude.

An estimate of the magnitude of seasonal fluctuations in ψ_{HT} is open to some discussion, and it could be that it is not sufficient for the west Pacific to exhibit

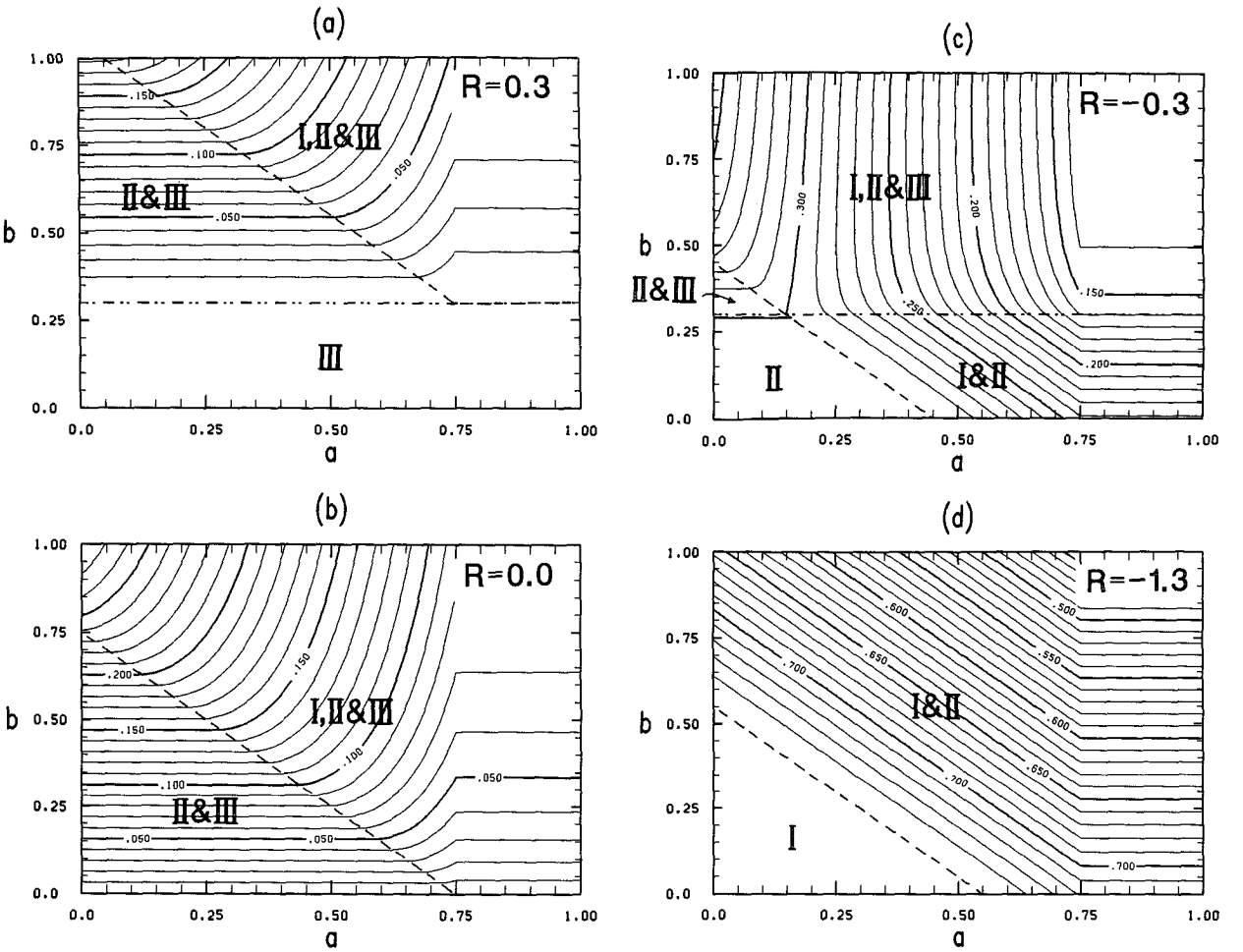

FIG. 6. As for Fig. 5 but including Halmahera, and where now R is reinterpreted as the mean value of ψ_{HT}. The mean value of ψ_H, $H = 0.75$ in all plots, and the perturbation amplitude of ψ_H, $h = a$ unless $a > H$, in which case $h = H$. The boundaries between regime regions are given by $b + h = |R + H|$ denoted by short dash and $b = |R|$ denoted by double dot-dash.

all three regimes during the year. An alternative scenario to the above is that horizontal mixing within the boundary currents is important, so that the freshness of the throughflow is determined by the amount of mixing between the SP component and the total NP water mass entering the seas, $-\psi_P$, assuming $\psi_P < 0$ for all time. Suppose $\psi_P \approx \psi_A$, and 40% of this NP water entering the Celebes Sea, that is, $0.4|\psi_A|$, goes to make up the throughflow in the absence of mixing. Further, suppose that $0.7|\psi_A|$ SP water from the SEC also enters the Celebes Sea, and $0.6|\psi_A|$ goes to make up the throughflow in the absence of mixing. If mixing in the Celebes Sea were complete, then the throughflow fraction would change from 40% NP–60% SP to 59% NP–41% SP.

4. A numerical GCM forced by realistic wind stresses

As stated earlier, different wind datasets produce different mean west Pacific Ocean states in a Sverdrup model. Meyers (1980) also questioned whether the NECC transport can be explained by Sverdrup dynamics. In the simple model, ψ_F is not restricted to that given by the Sverdrup transport; more realistic profiles could be chosen. In the tropics, the upper-ocean response to seasonally varying winds is dominated by baroclinic equatorial Rossby and Kelvin wave propagation. Based on sea-level data from various island stations, Wyrtki (1974) concluded that the seasonal variations in the NEC and NECC are in phase. Their amplitudes are a maximum from September to December, and a minimum from March to May. He also concluded that the SEC and undercurrent were in phase with each other, but 180° out of phase with the NEC and NECC. The Mindanao Current varies such that it is a maximum in the Northern Hemisphere winter. Philander et al.'s (1987) GCM simulation produced surface currents that were most intense when the undercurrent transport was a minimum in the Northern

Hemisphere fall and weak when the undercurrent transport was a maximum in spring. They also found considerable intraseasonal variability in the currents of the west Pacific, in particular in the SEC and very complex vertical structures. At this stage, instead of constructing a suitable ψ_F to model seasonal variations in composition, it is worthwhile to investigate further the ocean states produced by climatological forcing and the effect of viscous boundary-layer dynamics.

In a flat-bottomed model of the Pacific and Indian oceans, the adjustment time scale for the barotropic mode is sufficiently rapid that the barotropic streamfunction will vary as the wind stress on time scales of a month or longer. Therefore, if forced by monthly mean wind stresses, the ocean will progress through a series of Sverdrup states that may be interpreted as the upper-ocean state for a full model forced by perpetual January, February, and so on, winds. Also, if the wind forcing is confined to just the Pacific, then Australia and the other islands can be reduced to thin rectangular islands spanning the actual latitudes of the islands. The result is shown in Fig. 7, which is of the annual-mean barotropic streamfunction field for a homogeneous, flat-bottomed Bryan–Cox GCM (Cox 1984). The model was forced by the zonal component of Hellerman and Rosenstein's (1983) monthly mean wind stresses averaged between 155°E and 80°W and applied to the west of Australia. The applied wind stress and its curl are shown in Fig. 8. Borneo and the Philippines are combined with the Asian continent, and the barotropic streamfunction is set to zero on its coastline. The longitudinal distance between the land features is the minimum permitted by the grid spacing—that is, 2° for a 1° × 1° model—in the absence of prognostic temperature and salinity equations.

The gyre patterns and magnitudes shown in Fig. 7 are similar to the annual mean Sverdrup solution calculated by Godfrey (1989). The monthly variations are shown in Fig. 9. The Mindanao low is a maximum, 38 Sv, and most southerly, 5°N, for March winds. It moves northwards and weakens to a minimum of 22 Sv in July. It attains a secondary maximum, 37 Sv, in its most northerly location, 12°N, for November winds. The SEC high is at its minimum of 12 Sv and at its most southerly point 15°S in January. It moves northwards in March, and attains a maximum of 36 Sv at 4°S in August. It weakens and moves southwards in October. The low associated with the East Australia Current has two distinct maxima. It attains a maximum of 70 Sv in March at its southernmost location of 44°S. It attains a minimum of 41 Sv at 30°S in May, and increases to a second maximum of 62 Sv at 25°S in July. It weakens to another minimum of 41 Sv in November at 30°S. It should be emphasized that Fig. 9

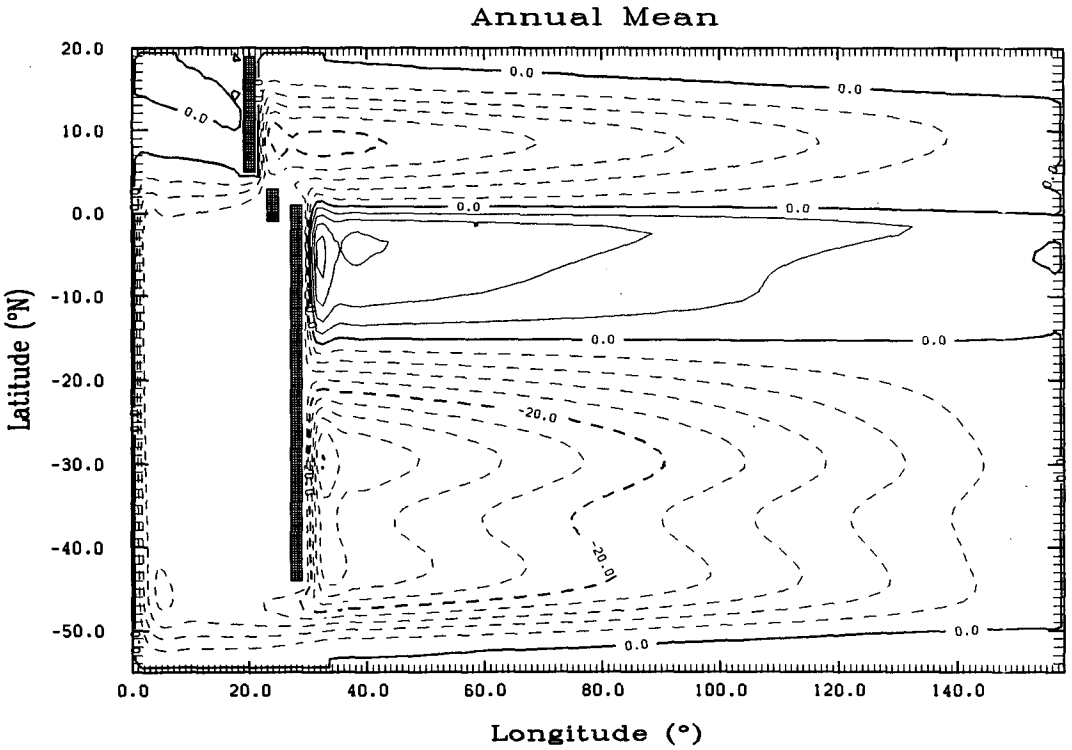

FIG. 7. The domain and geometry of the homogeneous, flat-bottomed GCM. The barotropic streamfunction field, averaged over an annual cycle, is contoured with interval 4 Sv.

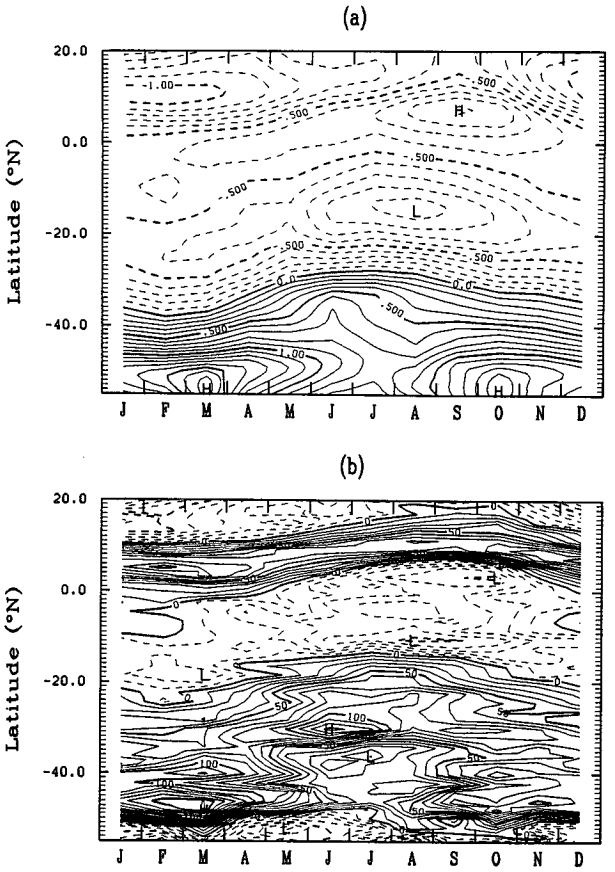

FIG. 8. The zonal component of wind stress from Hellerman and Rosenstein (1983) was averaged over the Pacific between 154.5°E and 79.5°W, and applied to the GCM west of Australia. The monthly variation is shown in (a) and the curl $\equiv -\partial\tau^x/\partial y$ in (b).

does not show seasonal variations in the pressure field of the upper levels. The plots are representative of the pressure field only if the model were forced by perpetual winds of a particular month. However, there are features similar to the observed seasonal variations in the surface currents. For example, the strength and southerly location of the Mindanao low in Fig. 9 in the Northern Hemisphere winter corresponds to that of the observed Mindanao dome, as described and modeled by Masumoto and Yamagata (1991). Similarly, the strengthening of the NECC and strengthening and more northerly location of the SEC high as the southeast trades intensify from May onward, Fig. 9, corresponds with observations and a realistic GCM simulation, as described by Philander et al. (1987).

The monthly variations in the circulation around Australia, and therefore the Indonesian Throughflow, are shown in Fig. 10a. It varies from a maximum of 16 Sv for March winds to a minimum of 9 Sv for August, which is counter to the supposed seasonal variation that has a maximum in August. This is because the effect of the monsoon winds has not been included. Also shown in Fig. 10a is the circulation around Halmahera, which lags that of Australia by about a month and has a much larger variation; its maximum is 19 Sv and its minimum is 6.5 Sv. The variation in ψ_A is much less than that of the lows and highs plotted in Fig. 10b. The viscous recirculation is estimated at O(5 Sv). Recirculation in western boundary layers, whether viscous or nonlinear, is identified by closed streamlines in Fig. 9, which imply that ψ_x is not of one sign in the boundary layer as assumed in the simple model of section 2. Due to the recirculation, the magnitude of the NECC in the GCM is not given by $\{\psi_1 - \psi_0\}$ but is considerably smaller. In the simple model, it was assumed that dissipation in a western boundary layer was sufficient to destroy at the latitude of creation the relative vorticity acquired by the parcel as it moves northward attempting to conserve its potential vorticity. Therefore, as the coastline curves from meridional to zonal, the boundary layer thins to zero. In the GCM, the vorticity is not wholly destroyed at the latitude of creation and a water parcel overshoots the latitude at which it eventually exits to rejoin the gyre; it spends longer in the boundary layer dissipating its vorticity. Comparing Fig. 9 with Figs. 1 and 2, the effect of the SEC overshooting y_N and the Mindanao Current overshooting y_P is that streamlines, which would otherwise enter the Celebes Sea and join those forming the NECC in a western boundary layer within the archipelago, join near the entrance in the west Pacific. This considerably reduces the amount of NP water flushing through the seas found in the simple model. However, in compensation, viscous effects lead to several streamlines from the SEC joining those forming the NECC in the region $y_N < y < y_P$. These streamlines forming the NECC would otherwise connect with ones from the Mindanao Current, which are now free to enter the archipelago and form the throughflow. Therefore, the GCM does not necessarily overestimate the freshness of the throughflow by having the SEC retroflect into the NECC; instead it produces a closure of the gyres that gives a compatibility between resolution, the large-scale current systems, and the throughflow and NECC compositions.

The magnitude of the throughflow for a given month agrees with Godfrey's Island Rule, (3.2), as shown in Fig. 11. There is a maximum deviation of 20% in September. The agreement was not expected to be good during the summer months when there is significant retroflection of SEC, so it is noteworthy that (3.2) still holds quite well. The agreement with (3.4) for the circulation around Halmahera is particularly poor for summer and fall conditions; then $|\psi_H|$ is over 100% larger than predicted, see Fig. 11. The meridional extent of Halmahera is not sufficient for frictional effects along its boundaries, excluding its eastern one, to be negli-

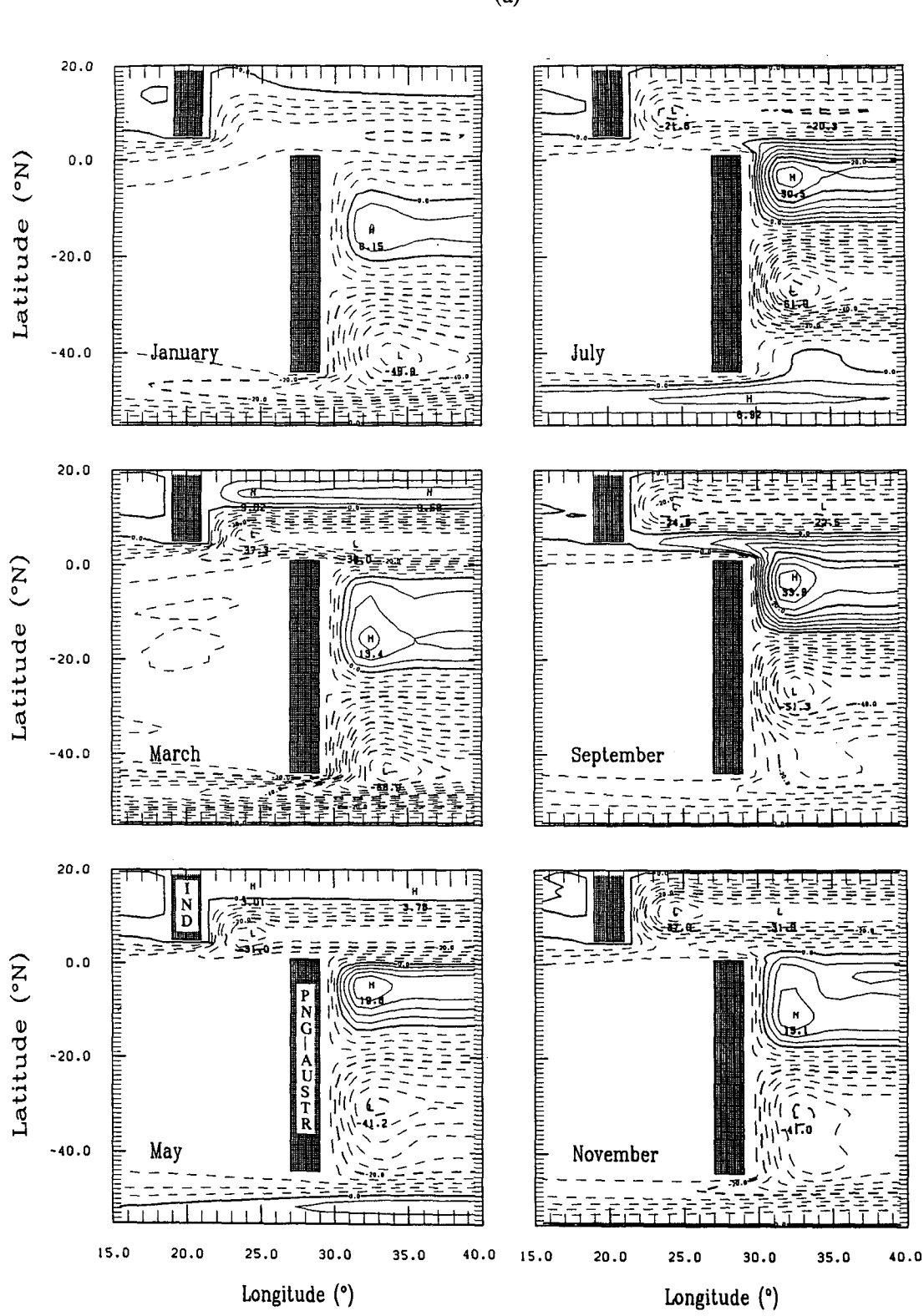

FIG. 9. Details of the streamfunction field showing (a) bimonthly variations in the Mindanao Current, SEC, and East Australia Current, and (b) monthly variations in the vicinity of the Indonesian basins.

(b)

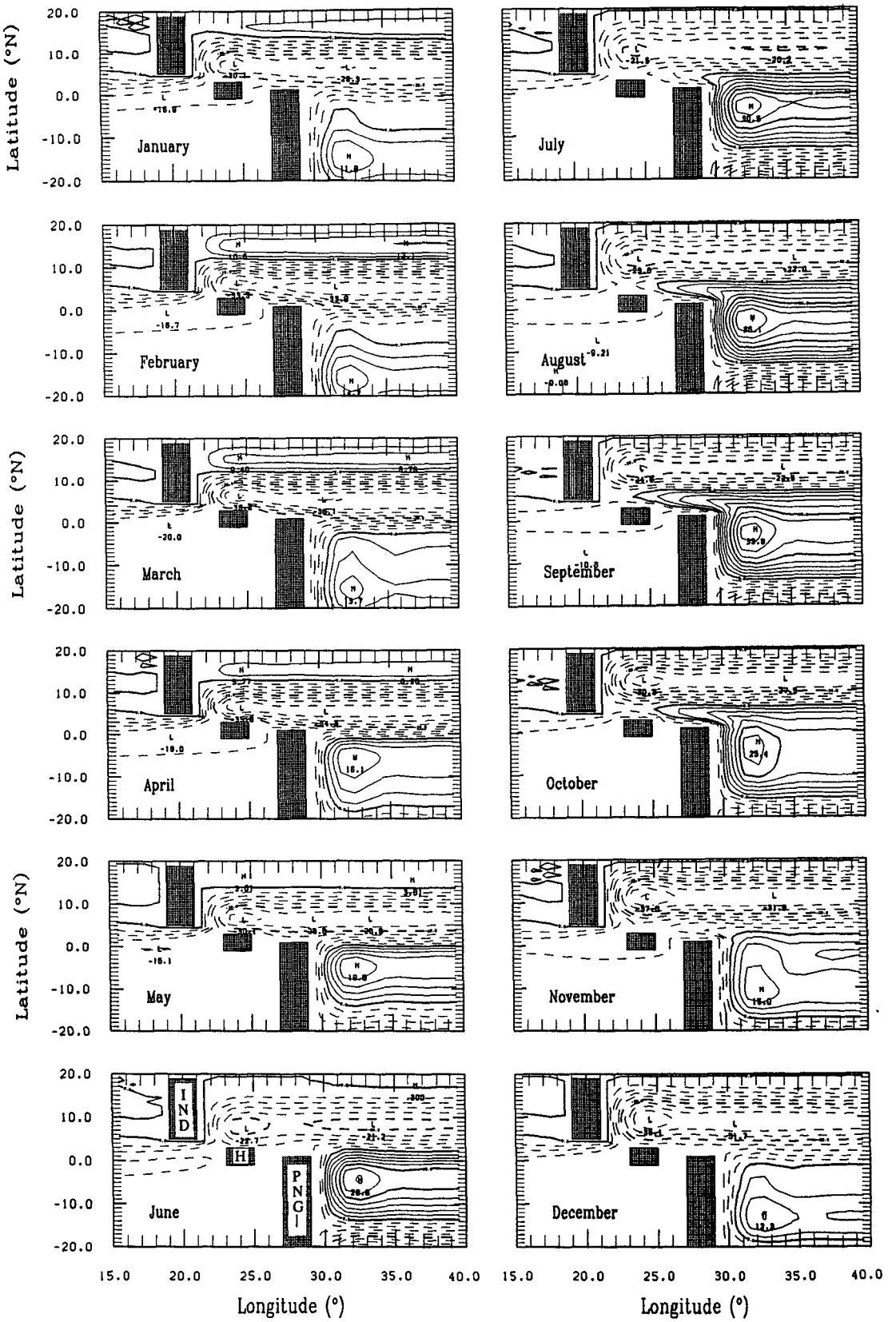

FIG. 9. (*Continued*)

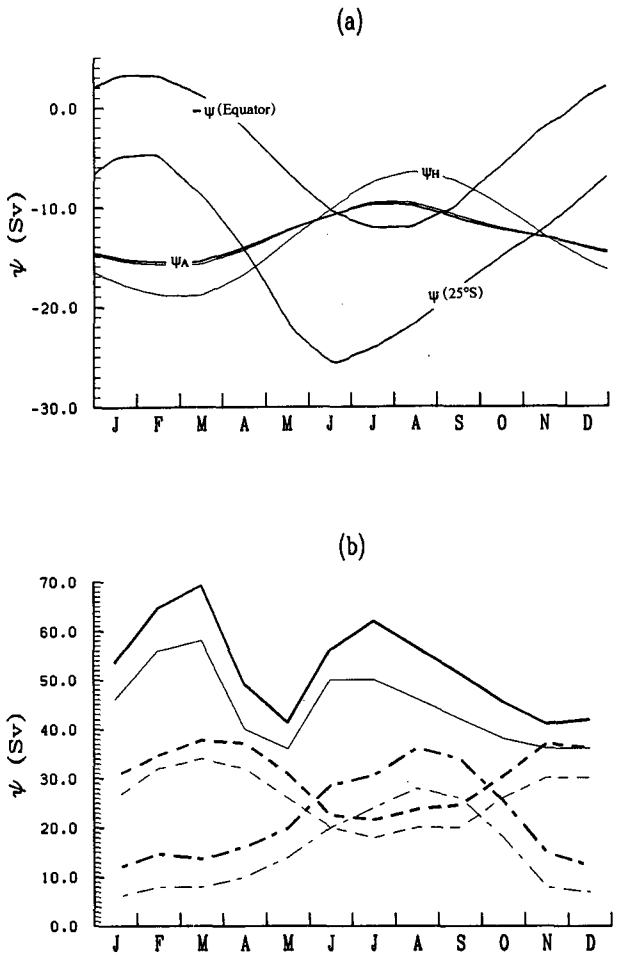

FIG. 10. The annual cycle of the barotropic streamfunction around Australia and Halmahera, and in the mid-"Pacific" on the equator and 25°S is plotted in (a). The field has been filtered (30-day running mean) to remove a free-basin mode of amplitude 2 Sv and period less than 10 days. The monthly variations in the Mindanao low (short dash) ($\equiv -\psi_0$), the SEC high (dot-dash) ($\equiv \psi_1$), and the EAC low (solid) ($\equiv -\psi_2$) are plotted in (b). The bold lines denote the actual values and the faint lines the values minus an estimate of the enhancement due to recirculation.

gible, which was assumed in deriving (3.4); see Wajsowicz (1993).

An estimate of the relative composition of the throughflow in terms of NP and SP waters is shown in Fig. 12a in the absence of Halmahera and in Fig. 12b including Halmahera. The regimes may be identified with those found in the simple model of section 2, though the transition criteria between regimes are slightly different due to viscous processes. For example, in the absence of Halmahera, it is not when $\psi_N > \psi_A$ that the throughflow is no longer of wholly NP origin, but when $\psi_F(y_N + \delta) > \psi_A$, where δ is a measure of the northward overshoot of the SEC past the northern tip of PNG, or rather the latitudes over which the SEC retroflects into the NECC; see Fig. 9a. For the model with Halmahera, the criterion $\psi_H > \psi_A$ for moving from regime I to II is robust, but once again the inequalities involving ψ_{HT}, ψ_N are not; there is significant viscous retroflection of the SEC into the NECC for July through November (see Fig. 9b). In the absence of viscous effects, regime III is predicted to occur for $\psi_N > 0$ in the absence of Halmahera, irrespective of the value of ψ_A, and so the ocean should be in this state for May through October winds. The effect of viscous retroflection is to shorten the time spent in regime III to August–October in the absence of Halmahera, and to September only if the model includes Halmahera. The meridional gradient in ψ_F is very large from May through October, and so the model is very sensitive to the overshoot, δ. In the latter half of the year, the meridional gradient in ψ is much weaker in the west Pacific, and the agreement with the criterion of the simple model for moving from regime III through to I is apparently much better.

The composition averaged over all 12 states for the two models is given in Table 3. Comparing Tables 3 and 1, it is notable that the NP component of the throughflow is much greater in both GCMs than in the simple model. This is because of the much longer time spent in regime I due to retroflection of the SEC, which also leads to less of a difference in averaged NP composition between the GCMs with and without Halmahera. In the simple model, the amount of time spent in regime I (regime III) during the cycle was 20% (40%) for NH1 and 40% (20%) for H1. In the context of Figs. 4 and 5 and the analysis of section 3b, $R \sim 0.6$, -1.6 for NH1 and H1, respectively, and $b \sim 2$, $a = 0 = h$, $H = 1$. Hence, the predicted NP compositions are quite disparate. In the GCM, the fraction of time in regime I is 50%, so the effective $R \sim -1$ for both models and the fractions are more similar. The time

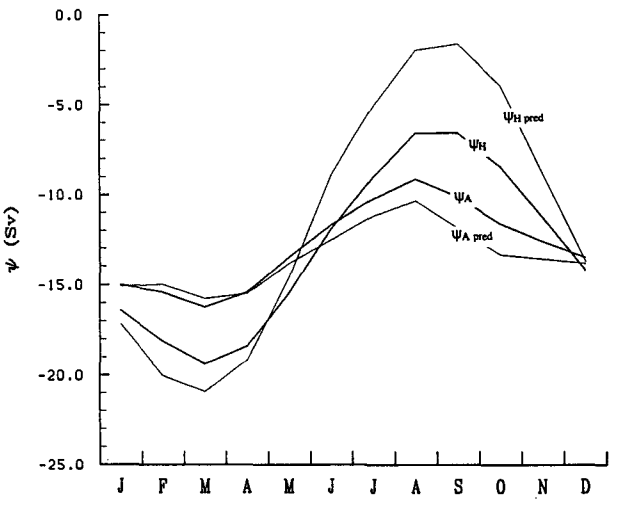

FIG. 11. The monthly variation in ψ_A, ψ_H, and theoretical estimates from (3.2) and (3.4), respectively.

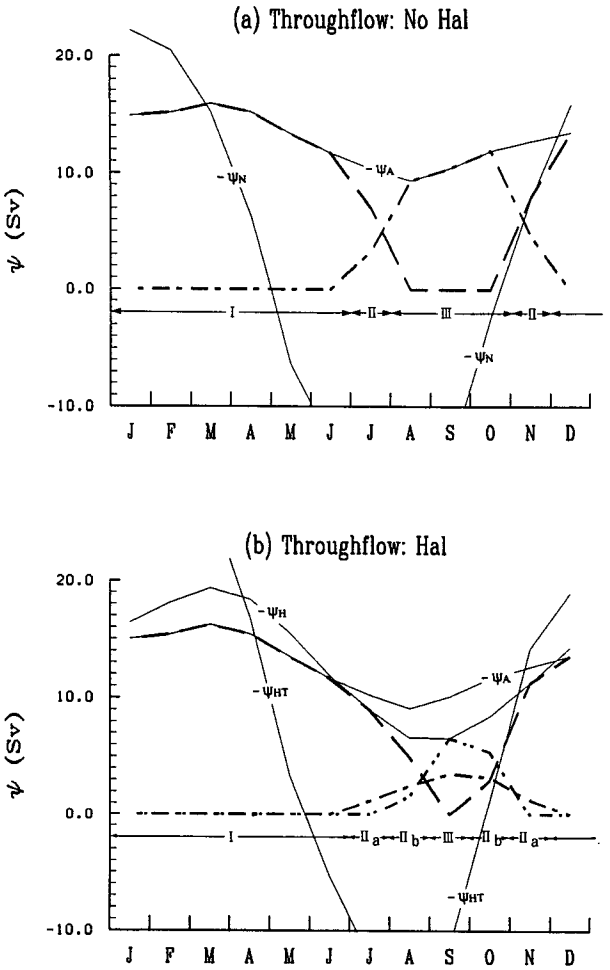

FIG. 12. An estimate of the throughflow composition in the GCM for (a) no Halmahera, (b) including Halmahera. The water masses distinguished are NP (long dash), SP (dot-dash), RSP (double dot-dash).

spent in regime III is only 25% (no Halmahera) and 8% (Halmahera), so $b \sim 1.4$, 1.0, respectively. From Fig. 11, $a \sim -0.16$ in both models, and $H \sim 0.8$ and $h \sim 2.6a$. These calculations imply that the amplitude of the perturbation to ψ_N or ψ_{HT}, b could be as large as O(1). In a Sverdrup model, the NECC spans about 2°S to 10°N depending on the season. In the real ocean, the NECC is confined between a pronounced ridge in the thermocline at about 10°N and a trough at 3°N, which coincides with the latitude of the northern tip of Halmahera. Therefore, variations in ψ_N, ψ_{HT} are not expected to be as large as the above implies.

An estimate of the variation in NECC composition in the two GCMs is shown in Fig. 13, and the average over the 12 states is given in Table 3. In contrast with the simple model, it is dominated by water fed directly from the Mindanao Current, 60% compared with 21%. In the simple model, there is a farther 25% (no Halmahera) of RNP—that is, water from the Mindanao Current—that has recirculated in the Indonesian Basin before exiting to feed the NECC. There is sufficient spatial resolution in the GCM to have the oppositely directed currents in the gap between the Philippines and PNG in the absence of Halmahera predicted by the simple model, as shown in Fig. 1. However, viscous effects are sufficient that the Mindanao Current separates at the southern tip of the Philippines and flows eastwards. In the model with Halmahera, there is not sufficient spatial resolution to have oppositely directed currents between the Philippines and Halmahera, so the excess water flushing through the Celebes Sea must exit south of Halmahera.

5. Discussion

A simple dynamical model, designed to give a qualitative description of the composition of the Indonesian Throughflow and NECC, has been presented. Given the value of the streamfunction for the depth-integrated flow on Australia–PNG and Halmahera, and its value at the interior edge of the western boundary layer at the northern tips of PNG and Halmahera and the southern tip of the Philippines, then the composition in terms of water masses directly fed from the Mindanao Current and SEC and fed after circulation within

TABLE 3. Estimate of composition in GCM averaged over an annual cycle.

	Throughflow (in Sv and percent of $\overline{\psi_{IT}}$)				
	NP	SP	RSP	$\overline{\psi_A}$	$\overline{\psi_H}$
No Halmahera	9.54 (74.3%)	3.30 (25.7%)	—	−12.84	—
Halmahera	10.75 (83.5%)	0.98 (7.6%)	1.14 (8.9%)	−12.87	−12.98
	$\overline{\psi_N} = -1.15$	$\overline{\psi_{HT}} = -8.03$			
	NECC (in Sv and percent of $\overline{\psi_{NECC}}$)				
	NP	SP	RNP		$\overline{\psi_{NECC}}$
No Halmahera	16 (39%)	24 (59%)	1 (2%)		41
Halmahera	14 (35%)	25 (62%)	1 (3%)		40

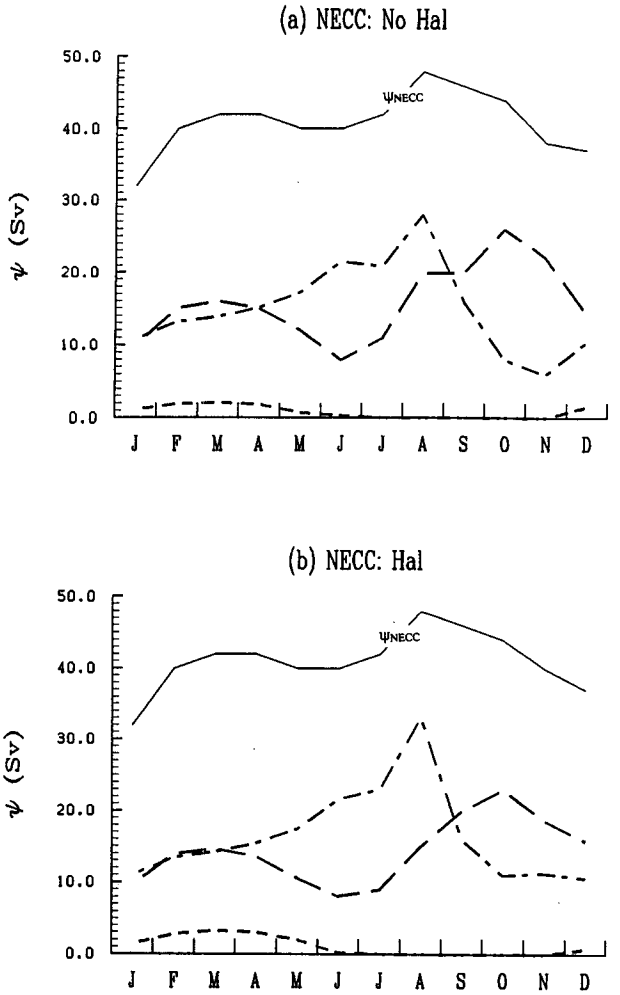

FIG. 13. An estimate of the NECC composition in the GCM. The water masses distinguished are NP (long dash), SP (double dot-dash), which includes WBL and RSP, and RNP (short dash).

the Celebes Sea is determined. The model does not determine the change in water mass properties due to either horizontal or vertical mixing in the Indonesian seas. Also, it does not take into account modifications to the streamline pattern west of the entrance into the Indonesian seas due to local wind forcing or topographic effects. The channels between Halmahera and the Philippines and PNG are wide and deep, so topographic effects are likely to be small in this region. Also, local wind forcing is unlikely to develop sufficient fetch to modify the streamline pattern significantly, but it will affect the magnitude of the circulation around Australia on seasonal time scales. Three principal composition regimes were identified. Typically, the throughflow is composed of water of wholly NP origin if the pressure in the equatorial west Pacific is low ($\psi_N \leq \psi_A$), and of wholly SP origin if it is high ($\psi_N \geq 0$); it is a mixture for intermediate values.

It is likely that the observed freshness of the throughflow is due to retroflection of the SEC into the NECC, as proposed by Godfrey et al. (1993), so giving a throughflow fed by the Mindanao Current. However, there are several other possibilities that have been explored here. First, Godfrey et al. (1993) did not take into account the small but important island of Halmahera, which spans the equator. Its inclusion leads to a revised estimate of 70% SP–30% NP for the throughflow composition. Second, there may be sufficient variability in the west Pacific on seasonal and interannual time scales that the system does not just exhibit the climatological mean gyre closures—that is, regime IIb—but spends time in regimes I and III. Third, in all the composition regimes of the simple model, there is a component of NP water that flushes through the Celebes Sea before exiting to make up the NECC. This could explain the apparent freshness of the Indonesian seas, and if sufficient mixing occurs, then it will contribute to the freshness of the throughflow. The total amount of NP water entering the Indonesian seas is given by the magnitude of the streamfunction at the interior edge of the western boundary layer at the southern tip of the Philippines—that is, ψ_P. Godfrey's (1989) Sverdrup streamfunction pattern from Hellerman and Rosenstein's (1983) wind-stress climatology would give 20 Sv total NP water entering the Indonesian basins, and 15 Sv of SP water in the absence of Halmahera, and about 10 Sv if Halmahera is taken into account. In practice, it could be ψ_P rather than ψ_{HT} that determines the throughflow freshness.

A simplified GCM was used to show different types of west Pacific Ocean states that could be generated by realistic wind stresses. The simple model predicts regime III of wholly SP origin for six months of the year. Viscous effects reduce this time to only one to three months with the system in regime I for six months. There is also a corresponding reduction in the component of the Mindanao Current flushing through the seas before exiting to make up the NECC.

The results are in broad agreement with the Lukas et al. (1991) buoy observations. Of buoys seeded in the Mindanao Current in June and tracked through September, three were advected directly into the NECC, two entered the Celebes Sea then exited into the NECC, two continued into the Makassar Strait. A further four buoys entered the Celebes Sea, but did not survive the measuring period. Of buoys released in the SEC, three buoys became entrapped in the Halmahera eddy, three entered the NECC before reaching the eddy, and one was grounded on Halmahera. Careful inspection of the Lukas et al. (1991) map reveals that all drifters were well north or east of the Halmahera–PNG entrance by the end of July, so it is not surprising that regime III was not found.

In conclusion, Gordon's (1986) annual-mean salinity calculation for the Indonesian region is not incon-

sistent with that which would be predicted by a Sverdrup model with simple western boundary-layer dynamics, but mixing within the Indonesian seas must be taken into account. Enough NP water is flushing through the basins, especially over the winter months, to give the required freshness. Halmahera's more northerly location is very important, and it should be included in any model of the region. Clarke (1991) has also emphasized the importance of the inclusion of Halmahera in the reflection and transmission of low-frequency waves. The regional geometry is also important. The connection between the Pacific and Indian oceans should be modeled as a series of basins connected by narrow straits within which mixing between various water masses can occur. If it is modeled as a wide passage, as in Godfrey (1989), then more complex dynamics must be invoked to explain the apparent freshness.

Acknowledgments. The author thanks Dr. Stuart Godfrey for introducing the problem to her. During the course of the research, the author was funded by a Japan Society for Promotion of Science research fellowship, and was on leave from a junior research fellowship at Wolfson College, University of Oxford. She would like to thank Prof. K. Takeuchi, Prof. T. Yamagata, and colleagues for their hospitality.

REFERENCES

Clarke, A. J., 1991: On the reflection and transmission of low frequency energy at the irregular western Pacific Ocean boundary. *J. Geophys. Res.*, **96**(Suppl.), 3289–3305.

Cox, M. D., 1984: A primitive equation, 3-dimensional model of the ocean. GFDL Ocean Group Tech. Rep. No. 1. Geophysical Fluid Dynamics Laboratory/NOAA, Princeton University, Princeton, NJ 08542.

Ffield, A., and A. L. Gordon, 1992: Vertical mixing in the Indonesian thermocline. *J. Phys. Oceanogr.*, **22,** 184–195.

Godfrey, J. S., 1989: A Sverdrup model of the depth-integrated flow for the world ocean allowing for island circulations. *Geophys. Astrophys. Fluid Dyn.*, **45,** 89–112.

——, A. C. Hirst, and J. Wilkin, 1993: Why does the Indonesian Throughflow appear to originate from the North Pacific? *J. Phys. Oceanogr.*, **23,** 1087–1098.

Goldenberg, S. B., and J. J. O'Brien, 1981: Time and space variability of the tropical Pacific wind stress. *Mon. Wea. Rev.*, **109,** 1190–1207.

Gordon, A. L., 1986: Interocean exchange of thermocline waters. *J. Geophys. Res.*, **91,** 5037–5046.

Hellerman, S., and M. Rosenstein, 1983: Normal monthly wind stress over the world ocean with error estimates. *J. Phys. Oceanogr.*, **13,** 1093–1104.

Hirst, A. C., and J. S. Godfrey, 1993: The role of the Indonesian Throughflow in a global ocean GCM. *J. Phys. Oceanogr.*, **23,** 1057–1086.

Kindle, J. C., H. E. Hurlburt, and E. J. Metzger, 1989: On the seasonal and interannual variability of the Pacific to Indian Ocean throughflow. *Proc. West Pacific Int. Meeting and Workshop on TOGA COARE,* Noumea, New Caledonia, 355–365.

Landsteiner, M. C., M. J. Mc Phaden, and J. Picaut, 1990: On the sensitivity of Sverdrup transport estimates to the specification of wind stress forcing in the tropical Pacific. *J. Geophys. Res.*, **95,** 1681–1691.

Lukas, R., E. Firing, P. Hacker, P. L. Richardson, and C. A. Collins, R. Fine, and R. Gammon, 1991: Observations of the Mindanao Current during the Western Equatorial Pacific Ocean Study. *J. Geophys. Res.*, **96**(Suppl.), 7089–7104.

Masumoto, Y., and T. Yamagata, 1991: Response of the western tropical Pacific to the Asian winter monsoon: The generation of the Mindanao Dome. *J. Phys. Oceanogr.*, **21,** 1386–1398.

Meyers, G., 1980: Do Sverdrup transports account for the Pacific North Equatorial Countercurrent? *J. Geophys. Res.*, **85,** 1073–1075.

Philander, S. G. H., W. J. Hurlin, and A. D. Siegel, 1987: Simulation of the seasonal cycle of the tropical Pacific Ocean. *J. Phys. Oceanogr.*, **17,** 1986–2002.

Sadler, J. C., M. A. Lander, A. M. Hori, and L. K. Oda, 1987: Tropical marine climatic atlas. Vol. II, Pacific Ocean. Tech. Rep. UHMET 87-02, Dept. of Meteorology, Univ. of Hawaii, Honolulu.

Semtner, A. J., and R. M. Chervin, 1988: A simulation of the global ocean circulation with resolved eddies. *J. Geophys. Res.*, **93,** 15 502–15 522.

Wajsowicz, R. C., 1993: The circulation of the depth-integrated flow around an island with application to the Indonesian Throughflow. *J. Phys. Oceanogr.*, **23,** 1470–1484.

Wyrtki, K., 1974: Sea level and the seasonal fluctuations of the equatorial currents in the west Pacific Ocean. *J. Phys. Oceanogr.*, **4,** 91–103.

——, 1987: Indonesian through flow and the associated pressure gradient. *J. Geophys. Res.*, **92,** 12 941–12 946.